Project Review Committee

Each research project has an advisory committee appointed by the LTRC Director. The Project Review Committee (PRC) is responsible for assisting the LTRC Administrator or Manager in the development of acceptable research problem statements, requests for proposals, review of research proposals, oversight of approved research projects, and implementation of findings.

LTRC appreciates the dedication of the following Project Review Committee members in guiding this research study to fruition.

LTRC Materials Administrator

Chris Abadie

Members

Sam Cooper, LTRC

Mike Boudreaux, DOTD

Doug Hood, LADOTD

Luanna Cambas, LADOTD

Philip Arena, FHWA

Directorate Implementation Sponsor

William H. Temple
DOTD Chief Engineer

TECHNICAL REPORT STANDARD PAGE

1. Report No. FHWA/LA04/391	2. Government Accession No.	3. Recipient's Catalog No.
4. Title and Subtitle Investigation of the Use of Recycled Polymer-Modified Asphalt in Asphaltic Concrete Pavements	5. Report Date June 30, 2004 6. Performing Organization Code LSU	
7. Author(s) Louay N. Mohammad, Ph.D., William H. Daly, Ph.D., Ioan I. Negulescu, Ph.D., Zhong Wu, Ph.D., P.E. and Codrin Daranga	8. Performing Organization Report No. LTRC 99-4B	
9. Performing Organization Name and Address Louisiana Transportation Research Center 4101 Gourrier Avenue Baton Rouge, LA 70808	10. Work Unit No. 11. Contract or Grant No. 736-99-1026	
12. Sponsoring Agency Name and Address Louisiana Transportation Research Center 4101 Gourrier Avenue Baton Rouge, La 70808	13. Type of Report and Period Covered Final Report 14. Sponsoring Agency Code LTRC and LEQSF	
15. Supplementary Notes		

16. Abstract

This report presents issues associated with recycling polymer modified asphalt cements (PMACs), particularly blending aged PMAC with new PMAC. A styrene-butadiene-styrene (SBS) PMAC was selected and graded using the Superpave Performance Grading (PG) protocol. Procedures were developed to separate the PMAC into its asphalt resin and polymer additive components and to characterize the relative concentrations of each component. Infrared spectrographic, thermogravimetric and rheological techniques were used to identify changes in the components as a result of aging. The impact of the extraction and recovery process on binder properties was found to be minimal. In this study, an SBS type elastomer PMAC meeting LADOTD specification for PAC-40HG and PG 70-22M was selected. A 19 mm nominal maximum aggregate size (NMAS) Superpave mixture was designed using virgin PAC-40HG blended with four different percentages (0, 20, 40 and 60 percent) of Reclaimed PMAC (RPMAC), and virgin aggregates. The RPMAC was extracted from lab-aged and field-aged asphalt mixtures. An eight-year-old field-aged PMAC binder was recovered from a wearing course mixture located on Route US61, Livingston Parish, Louisiana. All binders were characterized with respect to their composition and rheological properties. Binders extracted from field cores revealed that the US61 binder was quite brittle at a low temperature as measured by both force ductility and bending beam tests. In addition, blends of the US61 extracted binder with virgin PMAC were prepared and analyzed. The resultant blends exhibited much stiffer properties than those produced from the corresponding concentrations of lab-aged PMAC, indicating that the Pressure Aging Vessel (PAV) procedure did not predict the field aging of PMAC binders. A 19 mm Superpave mixture containing blends of virgin PMAC with various percentages of lab-aged and field-aged PMAC binders and original aggregates was evaluated by a suite of fundamental engineering tests including beam fatigue, indirect tensile strength and strain (ITS), indirect tensile creep, Asphalt Pavement Analyzer rut (APA), and repeated shear at constant height (RSCH). Test results indicated that as the percentage of RPMAC binder in mixtures increased, the rutting resistance increased, but the fatigue resistance decreased. Both the rutting factor of $G^*/\sin(\delta)$ at a high temperature and the fatigue parameter of $G^* \sin(\delta)$ at an intermediate temperature of the Superpave binder correlated fairly well with the results of mixture performance tests.

17. Key Words Polymer Modified Asphalt Cement, Recycled Polymer Modified Asphalt Cement. Aging, FTIR, GPC, rheology, Semi Circular Bend Test, Beam Fatigue, APA, FSCH, RSCH	18. Distribution Statement Unrestricted. This document is available through the National Technical Information Service, Springfield, VA 21161.

19. Security Classif. (of this report) N/A	20. Security Classif. (of this page) None	21. No. of Pages xii plus 72	22. Price **N/A**

INVESTIGATION OF THE USE OF RECYCLED POLYMER MODIFIED ASPHALT IN ASPHALTIC CONCRETE PAVEMENTS

By

Louay N. Mohammad, Ph.D.
Associate Professor, Civil and Environmental Engineering, Louisiana State University
Director, Engineering Materials Characterization Research Facility

William H. Daly, Ph.D.
Professor, Department of Chemistry, Louisiana State University

Ioan I. Negulescu, Ph.D.
Professor, Department of Human Ecology, Louisiana State University

Zhong Wu, Ph.D., P.E.
Material Research Associate, Louisiana Transportation Research Center

Codrin Daranga
Ph.D. candidate, Department of Chemistry, Louisiana State University

LEQSF (1998-01)-RD-B-04
LTRC Project No. 99-4B
State Project No. 736-99-1026

Conducted for

Louisiana Department of Transportation and Development
Louisiana Transportation Research Center

June 2004

ABSTRACT

This report presents issues associated with recycling polymer modified asphalt cements (PMACs), particularly blending aged PMAC with new PMAC. A styrene-butadiene-styrene (SBS) PMAC was selected and graded using the Superpave Performance Grading (PG) protocol. Procedures were developed to separate the PMAC into its asphalt resin and polymer additive components and to characterize the relative concentrations of each component. Infrared spectrographic, thermogravimetric and rheological techniques were used to identify changes in the components as a result of aging. The impact of the extraction and recovery process on binder properties was found to be minimal.

In this study, an SBS type elastomer PMAC meeting LADOTD specification for PAC-40HG and PG 70-22M was selected. A 19 mm nominal maximum aggregate size (NMAS) Superpave mixture was designed using virgin PAC-40HG blended with four different percentages (0, 20, 40 and 60 percent) of Reclaimed PMAC (RPMAC), and virgin aggregates. The RPMAC was extracted from lab-aged and field-aged asphalt mixtures. An eight-year-old field-aged PMAC binder was recovered from a wearing course mixture located on Route US61, Livingston Parish, Louisiana. All binders were characterized with respect to their composition and rheological properties. Binders extracted from field cores revealed that the US61 binder was quite brittle at a low temperature as measured by both force ductility and bending beam tests. In addition, blends of the US61 extracted binder with virgin PMAC were prepared and analyzed. The resultant blends exhibited much stiffer properties than those produced from the corresponding concentrations of lab-aged PMAC, indicating that the Pressure Aging Vessel (PAV) procedure did not predict the field aging of PMAC binders.

A 19 mm Superpave mixture containing blends of virgin PMAC with various percentages of lab-aged and field-aged PMAC binders and original aggregates was evaluated by a suite of fundamental engineering tests including beam fatigue, indirect tensile strength and strain (ITS), indirect tensile creep, Asphalt Pavement Analyzer rut (APA), and repeated shear at constant height (RSCH). Test results indicated that as the percentage of RPMAC binder in mixtures increased, the rutting resistance increased, but the fatigue resistance decreased. Both the rutting factor of $G^*/\sin(\delta)$ at a high temperature and the fatigue parameter of $G^* \sin(\delta)$ at an intermediate temperature of the Superpave binder correlated fairly well with the results of mixture performance tests.

ACKNOWLEDGMENTS

This study was supported by funds from the Louisiana Education Quality Support Fund (LEQSF), the Louisiana Transportation Research Center (LTRC), and the Louisiana Department of Transportation and Development (LADOTD). The authors would like to thank to all those who provided valuable help in this study. The financial and technical support of Koch Materials, Inc. of Wichita, Kansas is gratefully acknowledged. Ionela Chiparus, doctoral candidate at the Louisiana State University in Baton Rouge, LA, is acknowledged for her assistance in the extraction and characterization of field aged asphalts.

IMPLEMENTATION STATEMENT

This study evaluated the fundamental engineering properties of recycled asphalt pavements containing polymer modified asphalt cement (PMAC). A 19 mm Superpave mixture was designed using virgin polymer modified asphalt cement blended with four different percentages (0, 20, 40 and 60 percent) of Reclaimed PMAC (RPMAC) from lab-aged and field-aged asphalt mixtures, and virgin aggregates. Chemical and rheological properties of virgin and aged PMACs were evaluated using analytical methods and Superpave binder characterization tests. In addition, mixture characterization was performed using the Superpave test protocols, indirect tensile strength and strain, resilient modulus, creep, semi-circular fracture and loaded wheel tests. Based on the findings of this research the following is recommended for implementation:

A. The extraction procedure that was developed for removing aged asphalt binder from the aggregate. This procedure can be conducted as follows:

In a typical run 2-3 Kg of mix is placed in a large Soxhlet apparatus and extracted with 2 L of toluene at reflux under nitrogen until the toluene solvent siphoning from the extraction chamber is clear (12 to 18 hrs). The solution of asphalt binder in toluene is cooled to room temperature and then filtered to remove most of the fine particles of sand present. The filtered solution is allowed to stand overnight, decanted, and concentrated under vacuum to approximately 0.5 L using a Büchi Rotavapor R200 rotary evaporator. The concentrated asphalt binder solution in toluene is evaporated to dryness, then dried for 36 to 48 hours in a vacuum oven first at room temperature (ca. 24 hrs), then at 50°C for 12 hrs and finally at 115-120°C for 12 hours. A yield of 60 to 90 g of dried asphalt cement is recovered from each batch. To ensure that all the solvent (toluene) is removed, a thermogravimetric analysis (TGA) was performed after each batch dried. Less than 0.1 percent of the sample evaporated at temperatures below 180°C.

B. The gel permeation chromatography procedures that were developed for separating the PMAC into its asphalt resin and polymer additive components. These procedures are useful in ascertaining the quality of PMAC purchased by LADOTD.

The molecular weight distribution of the asphalt components including the polymer additive is estimated by using a gel permeation chromatograph. The separation of the polymer from the asphalt components is effected with two Phenogel 10 µ, 300 x 7.8 mm columns (Phenomenex, Torrance, CA), connected in series (1) 10-5 Å (10 K - 1,000 K); (2) MXM (5 K – 500 K). The column set is calibrated with narrow molecular weight polystyrene

standards. All samples are prepared at a concentration of two percent in tetrahydrofuran (THF) and 100 µL samples are injected at room temperature. Samples are eluted with THF at 0.8 mL/min and the polymer concentration in the eluent is recorded using a differential refractometer. The parent AC-30 elutes in a relatively broad band centering at an elution volume of 27.9 mL which corresponds to a molecular weight of ~1000 Daltons. The SBS sample elutes at 20.95 mL, which corresponds to a molecular weight of 110,000 Daltons. The large differences in the molecular weights between the asphalt and polymer components allowed baseline separation of the two peaks. The relative area under each peak corresponds to the relative concentrations of the two components.

C. The design method of the use of RPMAC as described in NCHRP report number 452 "*Recommended Use of Reclaimed Asphalt Pavement in the Superpave Mix Design Method: Technician's Manual*."

The following six steps were followed to determine the physical properties and critical temperatures of the RAP binder.

(1) Original DSR testing was performed on the recovered RAP binder to determine the critical high temperature, $T_c(High)$, based on original DSR values where $G^*/\sin\delta = 1.00$ kPa. The critical high temperature was calculated as follows:

(1.1) The slope of the stiffness-temperature curve was determined as $\Delta\text{Log}(G^*/\sin\delta)/\Delta T$.

(1.2) $T_c(High)$ was determined to the nearest 0.1°C using the following equation:

$$T_c(High) = \{[\text{Log}(1.00) - \text{Log}(G1)]/a\} + T_1 \qquad \text{eq. 1}$$

Where:

G_1 = the $G^*/\sin\delta$ value at a specific temperature, T_1, and

a = the slope of the stiffness–temperature curve described in (1.1).

The G*/sin d value closest to the criterion (1.00 kPa) is been used to minimize extrapolation errors.

(2) RTFO aging is performed on the remaining RAP binder.

(3) DSR testing is performed on the RTFO-aged recovered RAP binder to determine the critical high temperature (based on DSR). The critical high temperature (based on DSR) was calculated as described above. The G*/sin d value closest to the criterion (2.20 kPa) has been used to minimize extrapolation errors.

(4) The critical high temperature of the recovered RAP binder was determined as the lower of the original DSR and RTFO DSR critical temperatures. The high-temperature performance grade of the recovered RAP binder was determined based on this single critical high temperature.

(5) Intermediate temperature DSR testing on the RTFO-aged recovered RAP binder was performed to determine the critical intermediate temperature, $T_c(Int)$, based on pressure aging vessel (PAV) DSR. The intermediate high temperature (based on DSR) was calculated as described above. The G*/sin d value closest to the criterion ((5000 kPa) kPa) has been used to minimize extrapolation errors.

(6) BBR testing is performed on the RTFO-aged recovered RAP binder to determine the critical low temperature, $T_c(S)$ or $T_c(m)$, based on BBR stiffness or *m*-value.

(6.1) The slope of the stiffness-temperature curve was determined as $\Delta\text{Log}(S)/\Delta T$.

(6.2) $T_c(S)$ was determined to the nearest 0.1°C using the following equation:

$$T_c(S) = \{[\text{Log}(1.00) - \text{Log}(S_1)]/a\} + T_1 \qquad \text{eq. 4}$$

Where:

S_1 = the *S*-value at a specific temperature, T_1, and

a = the slope of the stiffness–temperature curve described in (6.1).

The S-value closest to the criterion (300 MPa) has been used to minimize extrapolation errors.

(6.3) The slope of the *m*-value-temperature curve was determined as $\Delta m\text{-value}/\Delta T$.

(6.4) $T_c(m)$ was determined to the nearest 0.1°C using the following equation:

$$T_c(m) = \{[\text{Log}(0.300) - \text{Log}(m_1)]/a\} + T_1 \qquad \text{eq. 5}$$

Where:

m_1 = the *m*-value at a specific temperature, T_1, and

a = the slope of the curve described in (6.3).

The m-value closest to the criterion (0.300) has been used to minimize extrapolation errors.

6.5 The higher of the two low critical temperatures $T_c(S)$ and $T_c(m)$ was selected to represent the low critical temperature for the recovered asphalt binder, $T_c(Low)$. The low-temperature performance grade of the recovered RAP binder was determined based on this single critical low temperature.

Blending Protocols

The maximum percentage of RAP that can be used in an asphalt mixture while still using the same virgin asphalt binder grade needs to be determined. Using the following equation for the high, intermediate, and low critical temperatures separately, the percentage of RAP needed to satisfy the assumptions can be determined.

$$\%\text{RAP} = (T_{\text{Blend}} - T_{\text{Virgin}})/(T_{\text{RAP}} - T_{\text{Virgin}}) \qquad \text{eq. 6}$$

TABLE OF CONTENTS

Abstract iii

Acknowledgments v

Implementation Statement vii

Table of Contents ix

List of Tables xi

List of Figures xiii

Introduction 1

Objectives 3

Scope 5

Methodology 7
- Materials 7
  - Asphalt binder 7
  - Asphalt mixture 7
  - Test factorials 7
- Material Characterization 11
  - Binder tests 11
    - Thermal analysis 11
    - FTIR spectroscopy 12
    - GPC characterization 12
    - Force ductility 12
    - DSR measurements 13
    - Bending beam rheometer measurements 13
    - Binder extraction procedure 13
  - Mixture Performance Tests 16
    - Indirect tensile stress (ITS) and strain test 17
    - Indirect tensile resilient modulus test 18
    - Indirect tensile creep test 19
    - Frequency sweep at constant height (FSCH) test 20
    - Repeated shear test at constant height 20
    - APA rut test 21
    - Semi-circular fracture test 21
    - Beam fatigue 22
  - Specimen Preparation 23

Discussion of Results 25
Binder Rheological Properties 25
Original (tank) PMAC binder 25
PMAC and Aged PMAC Blends 26
PMAC and Field-Aged PMAC Blends 28
Binder Extraction and Recovery 29
Fractionation of PMAC Binder 31
Characterization of Binder by Chemical Analyses 32
FTIR 32
Gel permeation chromatography 37
Differential scanning calorimetry 47
Force ductility 52
Mixture Characterization 54
Indirect tensile strength and strain test 54
Axial creep test 55
Indirect tensile resilient modulus test 56
Indirect tensile creep test 56
Asphalt pavement analyzer (APA) rut tester 57
Frequency sweep test at constant height 57
Repeated shear test at constant height 58
Simple shear test at constant height 59
Semi-circular fracture test 60
Beam fatigue test 62
Effects of Binder Performance Characteristics on Mixture Performance 63
Permanent deformation 63
Fatigue cracking 65
Development of Nomograph for blending RPMAC 66
RAP testing protocol 66
Blending Protocols 69
Application of Nomograph 69

Summary and Conclusions 71

Recommendations 75

List of Acronyms / Abbreviations / Symbols 77

References 79

LIST OF TABLES

Table 1. Asphalt cement specifications meeting LADOTD PAC-40 HG 8

Table 2. Asphalt cement specifications meeting Superpave PG 70-22 9

Table 3. Job mix formula 10

Table 4. Mixture performance tests 11

Table 5. Engineering property tests and protocols 17

Table 6. Original AC-30 binder rheological characterization 25

Table 7. Rigidity test results 26

Table 8. Rheological data for blends of PMAC with PAV-aged PMAC 27

Table 9. Viscosity of blends of PMAC with PAV-aged PMAC 27

Table 10. Rheological data for blends of PMAC with US-61S 29

Table 11. Elastic character of binders at high temperatures as reflected by the value of the storage modulus G' = G* cosδ at 80°C 31

Table 12. Thermal transitions of asphalt binders 52

Table 13. Comparison of the Critical Fracture Resistance for various asphalt mixtures 60

Table 14. Critical temperatures and performance grading of asphalts for recycling of US 61C asphalt pavement in a new asphalt composition……..…. 70

LIST OF FIGURES

Figure 1. Schematic presentation of the autoclave for SCF extraction..... 13

Figure 2. Temperature dependence of the modulus of rigidity of PMAC samples before (original) and after extraction in supercritical conditions (SCF extracted). 14

Figure 3. Soxhlet apparatus for extraction of asphalt using toluene 15

Figure 4. Rotary evaporator for concentration of toluene asphalt extracts 15

Figure 5. Percent weight loss versus temperature for PMAC sample 16

Figure 6. Typical curve of indirect tensile creep modulus vs. time 19

Figure 7-1. APA rut depth vs. load cycles 21

Figure 7-2. The Set-up of Semi-Circular Fracture Test 22

Figure 8. Creep and creep stiffness determined at -12°C for PAV aged PMAC blends containing *a priori* PAV aged PMAC material 28

Figure 9. Temperature / stiffness relationship of different binders 30

Figure 10. Variation of sinδ with temperature of the AC-30, PAC-40, PAV-aged PAC-40 and the binder extracted from the long-term aged mix containing PAC-40..... 31

Figure 11. Principle of an FTIR instrument 33

Figure 12. FTIR spectra of PMAC components and of polymer spiked PMAC (film on NaCl plate)..... 34

Figure 13. Comparative FTIR spectra of original and aged AC-30 asphalt samples (films on NaCl plates)..... 35

Figure 14. Comparative FTIR spectra of the original and aged PMAC samples (films on NaCl plates)..... 36

Figure 15. Comparative FTIR spectra of blends made with PMAC containing 20, 40, and 60 percent US61 binder (films on NaCl plates) 36

Figure 16. Schematic illustration of a GPC apparatus: *A*, solvent reservoir; *B*, solvent pump; *C*, injection valve; *D*, GPC column; *E*, detector; F, waste solvent/solution reservoir; and *G*, computer..... 37

Figure 17. Close-up of a column packing showing the pores 37

Figure 18. Principle of GPC: Larger size molecules excluded from pores 38

Figure 19. Schematic of a size-exclusion chromatography (GPC) column 38

Figure 20. Depiction of transit pathways of various sized molecules. …… 39

Figure 21. Building of a GPC chromatogram based on elution volume (time) 39

Figure 22. General scheme for a GPC experiment 40

Figure 23. Individual polymer molecules in diluted solutions 40

Figure 24. Aggregated polymer molecules formed in concentrated solutions 41

Figure 25. Crosslinked polymer molecules 41

Figure 26. GPC elution peaks of the base asphalt cement for PMAC (A), SBS polymer (B), 1:1 blend of base asphalt and SBS (C), and PMAC samples 42

Figure 27. GPC chromatogram of a blend of 3% SBS with AC-30 after TFOT…… 43

Figure 28. GPC elution peaks of the base asphalt cement for PMAC, PAV aged PMAC, and US-61S binder sampled from the road surface 44

Figure 29. GPC curves at low elution volumes (i.e., high MW) for PMAC, PAV aged PMAC and US-61S binder samples 44

Figure 30. Deconvoluted GPC curves of PMAC, PAV PMAC and US-61S binders 45

Figure 31. GPC curves for PMAC and its TFOT and PAV aged species 46

Figure 32. GPC curve of the binder extracted from the US-61C core sample taken from beneath the road surface plotted vs. the MW calibration scale 46

Figure 33. Deconvoluted GPC curve of the binder extracted from the US-61C core sample taken from beneath the road surface showing the peak corresponding to polymeric species 47

Figure 34. DSC thermogram of AC-30 material 48

Figure 35. Comparative DSC data of AC-30 and PMAC materials (Traces were normalized to 10 mg for quantitative representation) 48

Figure 36. DSC thermogram of SBS styrene-butadiene block copolymer 49

Figure 37. Glass transition and paraffinic crystallinity of PAV aged PMAC 51

Figure 38. Glass transition and paraffinic crystallinity of US-61S binder 51

Figure 39. Paraffinic crystallinity of US-61S binder and of the blend containing 40 percent US-61S binder and 60 percent PMAC 51

Figure 40. Force ductility data at different temperatures for US-61C binder..... 53

Figure 41. Indirect tensile strength and strain results 54

Figure 42. Toughness index..... 54

Figure 43. Creep stiffness and slope results from axial creep tests 55

Figure 44. Permanent deformation in axial creep tests 55

Figure 45. Indirect resilient modulus test 56

Figure 46. Indirect tensile creep test results..... 56

Figure 47. APA rutting test results 57

Figure 48. FSCH test results 58

Figure 49. Permanent shear strain from RSCH test..... 58

Figure 50. Permanent shear strain from SSCH tests 59

Figure 51. Maximum shear strain from SSCH tests 59

Figure 52. Variation of Fracture Energy with north depth 60

Figure 53. Fatigue test result (lab-aged RPMAC) 62

Figure 54. Fatigue test result (lab-aged RPMAC) 63

Figure 55. G/sin(δ) of binder vs. APA rut depth 64

Figure 56. G/sin(δ) of binder vs. creep slope in ITC test..... 64

Figure 57. G/sin(δ) of binder vs. permanent shear strain in RSCH test 65

Figure 58. G*sin(δ) of binder at 25°C vs. toughness index..... 66

INTRODUCTION

Asphalt cement for paving applications has been used for centuries. However, asphalt's intrinsic properties, such as low temperature cracking, fatigue cracking, permanent deformation at high temperature, and age hardening, limit the use of unmodified asphalt cement on today's highly demanding routes [1]. Therefore, the use of polymer modified asphalts has increased steadily over the last several years because they have improved intrinsic properties of asphalt binders and resulted in better-performing pavements [2-5]. In many states, polymer modified asphalt cements (PMACs) have been specified for all new road construction. The wearing characteristics of PMACs have been excellent, but many of the initial PMAC placements are reaching the end of their lifetimes and resurfacing must be scheduled.

Recycled asphalt pavements (RAP) are not new to the highway industry. As early as the 1930s, there were reports on the use of RAP [6]. It was not, however, until the mid- to late-1970s that the hot mix asphalt (HMA) recycling became popular [7]. Today, with the increase of construction prices (raw materials like asphalt and aggregates) and the environmental awareness, the use of recycled pavements has become more and more important. Sources suggest that, every year, more than 45 million tons of HMA are being removed from waste pavements in the United States [8]. Reconstructing the pavements requires about the same amount of raw materials. If the waste HMA is simply disposed, large quantities of raw aggregates need to be transported from various sources, necessitating more land fills to accommodate the wastes. Using RAP makes use of materials that would otherwise be disposed of usually as landfill, reduces the demand for new sources of material (quarries and asphalt binder), and, in many cases, reduces construction costs. RAP is beneficial in reducing the cost of both highway construction and environmental protection. Therefore, some states have imposed rules that require a certain percentage of waste pavements be recycled. Currently in Louisiana, 100 percent of reclaimed asphalt pavement materials are being recycled for highway usage in one form or another. Although RAP can be used for various purposes such as granular shoulders, embankments, or any form of filling materials, the most preferred usage is as an asphalt bound layer somewhere in the pavement structure.

The Louisiana Department of Transportation and Development (LADOTD) has adopted the use of polymer modified asphalt cement (PMAC) in most of its hot mix asphalt mixtures since 1994. Little research has been conducted on recycling PMAC pavements because there was not an urgent need then. However, as more and more PMAC pavements are being constructed, this problem has become more realistic and needed. Louisiana's first PMAC

pavements were built in the late 1980s. These pavements have already approached the time for rehabilitation. To fully utilize the potential of waste material, it is necessary to evaluate the fundamental characteristics of recycled polymer modified asphalt pavements and develop a practical procedure for designing and constructing flexible pavements using them.

Adding appropriate polymers to asphalt binders can significantly improve the performance of asphalt concrete pavements, e.g., increasing fatigue cracking resistance, reducing the extent of permanent deformation, improving thermal cracking resistance, minimizing moisture sensitivity, and potentially reducing age hardening [9, 10]. These positive contributions have prompted a number of state transportation departments to require that polymer be incorporated into all asphalt pavements. The predominant polymers incorporated in asphalt cements are elastomers such as styrene-butadiene rubber (SBR) [11, 12] or styrene-butadiene-styrene (SBS) block copolymers [13].

The extensive use of PMACs improves asphalt pavement performance. However, several critical questions associated with the recycling of PMACs remain to be answered. It has been reported that some additives in asphalt mixtures caused difficulties during recycling. For example, latex rubber modified asphalt mixes tend to gum up the teeth on the milling machine. Sulfur enriched asphalt mixes release toxic fumes during the process of re-heating [7, 14]. Clearly, such issues need to be answered before recycled polymer modified asphalt mixtures can be accepted by the industry. These questions can be summarized as follows:

- Will the polymer additives degrade or harden during long term exposure to field conditions and thus no longer contribute to the binder properties?
- What fundamental material characteristics will the binder and mixes have at different percentages of recycled polymer modified asphalt mixes?
- How can the binder consistency be adjusted in recycled-virgin asphalt blends to restore the properties of PMACs?

The aim of this project is to address the potential problems of recycling polymer modified asphalt mixtures.

OBJECTIVE

The objectives of this research were to (1) analyze the properties of field-aged PMAC relative to Pressure Aging Vessel (PAV) aged PMAC; (2) examine the compatibility and feasibility of blending reclaimed PMAC with virgin PMAC based on chemical component analysis methods and Superpave binder specification; and (3) evaluate the fatigue and permanent deformation properties of asphalt mixtures containing various percentages of laboratory-aged and/or field-extracted PMACs based on laboratory fundamental engineering tests.

SCOPE

This project was divided into three phases encompassing binder study, mixture study, and a finalized design procedure. During Phase I (binder study), extraction techniques were developed for separating the asphalt from the polymer additive and removing aged asphalt binder from the aggregate in asphalt mixtures. Binder tests were based on a chemical component analysis and Superpave binder characterization, which included (1) differential scanning calorimetric (DSC) measurement, (2) Fourier transform infrared (FTIR) measurement, (3) gel permeation chromatograph (GPC) measurement, (4) rotational viscosity measurement, (5) dynamic shear modulus and phase angle measurement, (6) beam stiffness and creep slope measurement. During Phase II and III, a typical LADOTD high volume mixture was selected and designed using virgin PMAC blended with different percentages of RPMAC (0, 20, 40 and 60 percent) and virgin aggregates. The RPMACs used in Phase II and Phase III studies were extracted in a chemistry laboratory from lab-aged and field-aged asphalt mixtures, respectively. A suite of fundamental engineering tests, including frequency sweep at constant height (FSCH), repeated shear at constant height (RSCH), simple shear at constant height (SSCH), indirect tensile strength and strain (ITS), indirect tensile modulus (M_r), semi-circular fracture, beam fatigue, and asphalt pavement analyzer (APA) tests, were conducted on both lab-aged and field-aged RPMAC mixtures.

METHODOLOGY

Materials

Asphalt Binder

A standard SBS elastomer PMAC meeting LADOTD specification for PAC-40HG and PG 70-22M was obtained from Koch Materials Company of Wichita, Kansas. The supplier also provided samples of the AC-30 asphalt and of the polymer additive Solprene. A visit to the local asphalt compounder in Donaldsonville helped the researchers to understand and duplicate the blending procedure. Tables 1 and 2 present the specification and test results for PAC-40HG and PG 70-22M, respectively. The original binder was short- and long-term aged to simulate in-service aging of binders. This binder is referred to hereafter as lab-aged RPMAC. An eight-plus years old asphalt binder was extracted from road samples taken from US61 Hwy (Livingston Parish, Louisiana). RPMAC samples obtained by surface bump grinding were designated as US-61S and those from field cores were labeled US-61C.

Asphalt Mixture

A 19 mm nominal maximum aggregate size (NMAS) Superpave mixture was selected in this study, representing a typical LADOTD high volume Superpave mixture. The aggregates used in this study were siliceous limestone obtained from Vulcan Materials Company, Reed Quarry in Gilbertsville, Kentucky. Table 3 shows the Job Mix Formula (JMF). The aggregate proportions for this mix were 25 percent No. 67; 25 percent No. 78; 45 percent No. 11; and 5 percent coarse sand. The optimum binder content selected at 4 percent air voids was determined from standard Superpave mix design. Specimens were prepared using the Superpave Gyratory Compactor (SGC) with initial-, design-, and final-number of gyrations of 9, 125, and 205, respectively. The optimum asphalt content at the design gyrations was determined to be 4.2 percent.

Test Factorials

Superpave physical tests on asphalt binder, including rotational viscometer, dynamic shear rheometer, and bending beam rheometer, were conducted on the virgin and both lab- and field- aged PMAC binders used in this study. Chemical analysis methods, such as DSC, FTIR and GPC, were also conducted on virgin and aged PMAC binders to identify the impact of the laboratory extraction methods developed in this study. In addition, Indirect Tensile Resilient Modulus (M_R), Indirect Tensile Strength (ITS) and Strain, Axial Creep, Indirect Tensile Creep, Semi-circular Fracture, Beam Fatigue, Superpave Frequency Sweep at Constant Height (FSCH), Repeated Shear at Constant Height (RSCH), Simple Shear at Constant Height (SSCH) and Asphalt Pavement Analyzer (APA) rut tests were performed to

characterize the fundamental engineering properties of Superpave mixtures with different RPMAC contents. Table 4 lists the performance tests proposed in this study and the corresponding number of specimens tested.

Table 1
Asphalt cement specifications meeting LADOTD PAC-40 HG

	SPECIFICATIONS	TEST RESULTS
Original Properties		
Viscosity, 140°F (60°C), Poises	Min. 4000	6629
Viscosity, 275°F (135°C), centistokes	Max. 2000	1200
Penetration, 77°F (25°C), 100 g, 5 s, min.	50 - 75	59
Flash Point, Cleveland open cup, min. °F (°C)	450 (232)	480
Solubility in trichloroethylene, min., %	99.0	99.9
Separation of Polymer, 325°F (163°C), 48 hrs Difference in softening point from top and bottom, max., °C	2.0	1.0
Force Ductility Ratio, (F_2/F_1, 39°F (4°C), 5 cm/min, @ 30 cm elongation, min.) F_2 = F @ 30 cm, F_1 = Peak Force	0.3	0.32
Test on residue from thin-film oven test		
Viscosity, 140°F (60°C), Poises Ductility, 77°F (25°C), 5 cm/min, min., cm Penetration Retention, min., % of original	- - 50	18524 - 38
Elastic Recovery, 25°C @ 10 cm elongation, % min.	60	65

Table 2
Asphalt cement specifications meeting Superpave PG 70-22

Test	**Property**	**Test Results**	**PG Criteria**
Original Binder			
Flash Point	N/A	-	230°C
Rotational Viscosity (Pa·s)	135°C @100 rpm	1.125	3 Pa·s, Max
Dynamic Shear Rheometer (kPa)	**G*/sin** d	@ 70°C 1.782 @ 76°C 1.029	1.0 kPa, Min
TFOT Aged Binder			
Mass Loss (%)	N/A	< 1.0	1% Max.
Dynamic Shear Rheometer (kPa)	**G*/sin** d	@ 70°C 3.232 @ 76°C 1.772	2.20 kPa, Min
PAV Aged Binder			
Dynamic Shear Rheometer (kPa)	**G*sin** d	@28°C 1036.3 @ 31°C 707.4	5000 kPa, Max.
Bending Beam Rheometer (-12°C)	Stiffness	110	300 MPa, Max.
Bending Beam Rheometer (-12°C)	M value	0.39	0.300, Min.
PG Grading		**70-22**	

Table 3
Job mix formula

Job Mix Formula	Mix	19.0 mm
	AC%	4.2%
	Aggregates	25% No. 67
		25% No. 78
		45% No. 11
		5% CS
Gradation % Passing	1” (25 mm)	100
	3/4” (19 mm)	96
	1/2” (12.5 mm)	82
	3/8” (9.5 mm)	65
	No. 4 (4.75)	45
	No. 8 (2.36)	32
	No. 16 (1.18)	23
	No. 30 (0.60)	15
	No. 50 (0.30)	9
	No. 200 (0.075)	5.2
G_{mb}	2.420	
G_{mm}	2.531	
%VMA @ N_{des}	13.4	
%VFA @N_{des}	67	
%Air Voids @ N_{des}	4.1	
% G_{mm} @N_{ini}	85	
% G_{mm} @N_{fin}	97	

Table 4
Mixture performance tests

Tests	Protocols	Engineering Properties	Mixtures							
			0% RPMAC		20% RPMAC		40% RPMAC		60% RPMAC	
			LA[1]	FA[2]	LA	FA	LA	FA	LA	FA
MR (5°C, 25°C, 40°C)	ASTM D 4123 (modified)	Elastic Properties (MR and μ)	3	3	3	3	3	3	3	3
ITS at 25°C	AASHTO T245	Durability and Fatigue Crack	3	3	3	3	3	3	3	3
IT Creep at 40°C	Mohammad et al (1993)	Permanent Deformation	3	3	3	3	3	3	3	3
Semi-circular Fracture at 25°c	Mull el al (2002)	Fracture Resistance	0	6	0	6	0	6	0	6
Beam Fatigue	SHRP M009	Fatigue Resistance	3	3	3	3	3	3	3	3
FSCH at 60 °C	AASHTO TP7	Viscoelastic Properties (G*,δ)	3	3	3	3	3	3	3	3
RSCH at 60°C	AASHTO TP7	Permanent Deformation	3	3	3	3	3	3	3	3
SSCH at 60°C	AASHTO TP7	Permanent Deformation	3[3]	3[3]	3[3]	3[3]	3[3]	3[3]	3[3]	3[3]
APA Rut at 64°C	Rut Susceptibility	Rut Susceptibility	3	3	3	3	3	3	3	3

[1] LA – Lab-aged; [2] FA – Field-aged; [3] SSCH tests used the tested FSCH specimens.

Material Characterization

A suite of binder composition, rheology, and mixture characterization tests was performed in this study. The section below briefly describes the binder and mixture tests conducted.

Binder Tests

Thermal Analysis. The glass transition and melting transitions of the binders were measured using differential scanning calorimetry (DSC). DSC was performed using both a Seiko 220 DSC and a Universal V2.6D TA instrument, both of which calibrated for temperature and enthalpy with indium. A typical DSC measurement was conducted on ≅ 10 mg sample sealed in an aluminum sample pan using a similar empty pan with cap as a

reference. Larger samples, up to 40 mg, were employed to estimate the Tg of the binders. These samples were heated to 80°C for 30 minutes to eliminate prior thermal history and quenched in liquid nitrogen before mounting in a DSC cell; measurements were initiated at -50°C.

FTIR Spectroscopy. The functional group composition of the binders was examined by qualitative Fourier Transform Infrared (FTIR) using a Perkin Elmer 1700 FTIR spectrophotometer. Films of asphalts and rubber were cast from toluene on a NaCl plate and analyzed taking the blank plate as background.

GPC Characterization. The molecular weight distribution of the asphalt components was estimated by using a gel permeation chromatograph (GPC) equipped with a Waters 590 pump and a Waters model 410 differential refractive index detector. The separation of the polymer from the asphalt components was effected with two Phenogel 10 µ, 300 x 7.8 mm columns (Phenomenex, Torrance, California), connected in series (1) 10-5 Å (10 K - 1,000 K) and (2) MXM (5 K – 500 K). The column set was calibrated with narrow molecular weight polystyrene standards. All samples were prepared at a concentration of two percent in tetrahydrofuran (THF) and 100 µL samples were injected at room temperature. Samples were eluted with THF at 0.8 mL/min and the polymer concentration in the eluent was recorded using a differential refractometer.

Force Ductility. This test was conducted in accordance with ASTM P226. A copper mold was coated with a release agent and molten asphalt was poured into it to form a dog-bone specimen with a 3 cm test area. The specimen in the mold was placed in a constant temperature bath set at 4 ± 1°C, allowed to equilibrate, and then the excess asphalt was trimmed from the specimen. The trimmed mold was replaced in the bath, re-equilibrated, and then the specimen was removed. The specimen was strained at 5 cm/min up to a maximum extension of 30 cm. The force required to apply the strain was plotted versus time. A normal test produced a chart record showing two peaks, with the second peak lower than the initial peak. The tensile stress ratio is defined as the force (f2) at the second peak divided by the force of the initial peak (f1). A sample passed the test if it stretched at least 1,000 percent.

DSR Measurements. A Bohlin CVO dynamic shear rheometer, DSR, specially designed for characterization of asphalt cements (Bohlin Instruments Div., Metric Group Inc., Cranbury, New Jersey) was used to investigate the rheological behavior of the virgin PMAC and field-recovered binder. This test was performed according to AASHTO TP5 [15] “Determining the

Rheological Properties of Asphalt Binder Using a Dynamic Shear Rheometer." The testing parameters were the following: measurement type - high temperature range; target temperature - different values; strain amplitude - 12.0 percent; plate diameter - 25.0 mm; plate gap - 1,000 µm (1.0 mm); and equilibration time - 3.0 min.

Bending Beam Rheometer Measurements. The bending beam rheometer (Cannon TEBBR) was used to measure the low-temperature creep response of PAV-aged binders. This test was performed in accordance with AASHTO TP1 [16]. Data was collected at six loading times (8, 15, 30, 60, 120 and 240 sec) for a load on the beam of 100 ± 5 g.

Binder Extraction Procedure. Extraction of asphalts from RPMAC should be complete in order to determine its physical properties for recycling purposes. The extraction method should not adversely affect the material; for example, oxidation should not occur during the extraction and/or concentration steps.

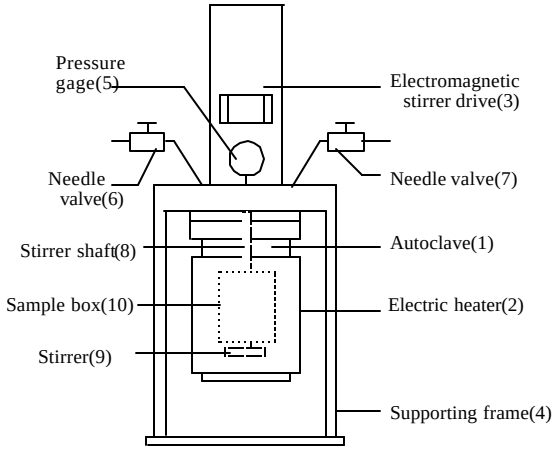

Figure 1
Schematic presentation of the autoclave for SCF extraction

The schematic presentation of the autoclave for the supercritical extraction procedure-SCF extraction used in this study is presented in Figure 1. The sample was extracted with a mixture of toluene (T) and dimethyl ether (DME) at a pressures and temperatures higher than the critical parameters for DME (53.7 atm and 126.9°C, respectively). In a typical extraction experiment, 2g of PMAC was introduced in sample box (10) which was made of a fine mesh stainless steel sieve, and was extracted with a mixture of T (200 g) and DME (50g) for 2 hours at 130-150°C and 700-800 psi (14.21 psi = 1 atm). The pressure was adjusted with argon compressed at 1,600 psi through the needle valve (6).

When the extraction was considered finished, the temperature was allowed to decrease to 20-30°C and the pressure was dropped to atmospheric conditions (≅1atm) by releasing both the argon and DME (DME boils at -15° C at 1atm) through the needle valve (7). The extract was concentrated in vacuum (100 mm Hg @ 95°C) using a rotary evaporator. The absence of the solvent in the extracted material was checked by thermogravimetry (*vide infra*) in inert nitrogen atmosphere at 150°C (T boils at 110°C at 1 atm) using a thermogravimetric (TG) balance. Furthermore, the rheological properties of the material extracted in SCF conditions were compared to those of the original PMAC to determine if the extraction process altered the material properties.

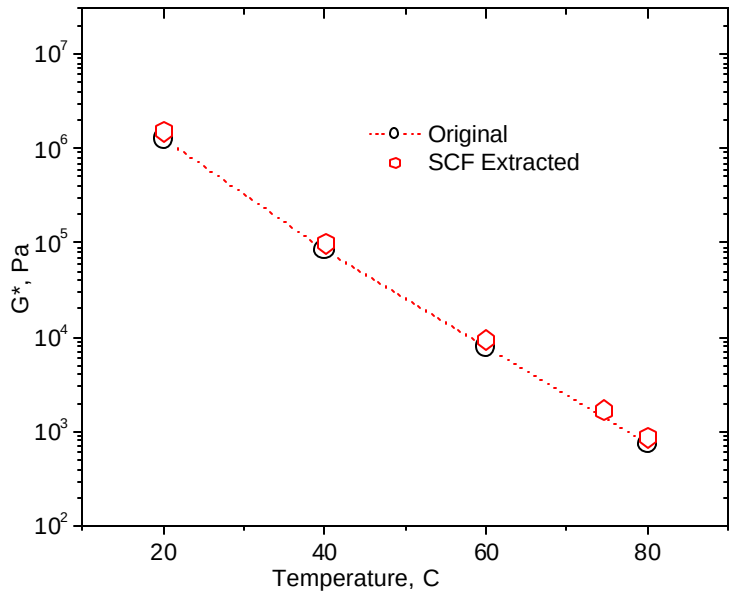

Figure 2
Temperature dependence of the modulus of rigidity of PMAC samples before (Original) and after extraction in supercritical conditions (SCF Extracted)

As shown in Figure 2, the complex modulus of rigidity G* of the extracted sample correlates very well with that of the original PMAC over the whole range of temperatures tested.

Since the SCF extract was completely soluble in toluene, extraction of the binder from the mix was also performed at atmospheric pressure using a Soxhlet apparatus (Figure 3) and hot toluene. A nitrogen blanket was applied to avoid oxidation. The extract was vacuum-filtered in order to separate the dust carried out by the flowing toluene and concentrated in vacuum (100 mm Hg @ 95°C) using a rotary evaporator (Figure 4). Furthermore, the solvent traces

were removed in a vacuum oven at 0.1 mm Hg and 95°C. The absence of the solvent in the extracted material was checked by thermogravimetry. In a typical experiment, 100g of mix was extracted using 500 ml of toluene. An average amount of 3g binder/100 g mix was extracted.

Figure 3
Soxhlet apparatus for extraction of asphalt using toluene

Based on these results, an efficient technique for the extraction of asphalt cements from mixtures was developed as follows.

Figure 4
Rotary evaporator for concentration of toluene asphalt extracts

In a typical run, 2-3 kg of mix was placed in a large Soxhlet apparatus and extracted with 2 L of toluene at reflux under nitrogen until the toluene solvent siphoning from the extraction chamber was clear (12 to 18 hrs). The solution of asphalt cement in toluene was cooled to room temperature and then filtered to remove most of the fine sand particles. The filtered solution was allowed to stand overnight, decanted, and concentrated under vacuum to approximately 0.5 L using the Büchi Rotavapor R200 rotary evaporator shown in Figure 4. The concentrated asphalt cement solution in toluene was then dried for 36 to 48 hours in a vacuum oven first at room temperature (ca. 24 hours), then at 50°C for 12 hours and finally at 115-120°C for the rest of the time. A yield of 60 to 90 g of dried asphalt cement was recovered from each batch. To ensure that all the solvent (toluene) was removed, a thermogravimetric analysis (TGA) was performed after each batch dried. A typical TGA curve is shown in Figure 5. Note that less than 0.1 percent of the sample evaporated at temperatures below 180°C.

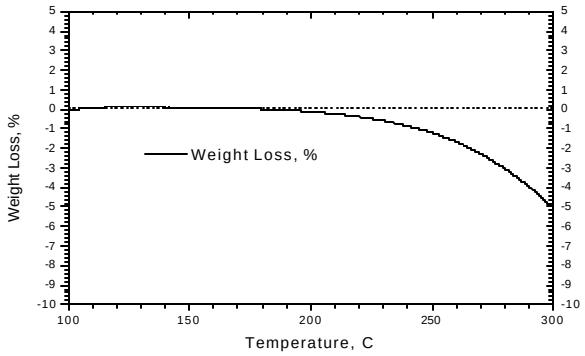

Figure 5
Percent weight loss versus temperature for PMAC sample

Mixture Performance Tests

A series of engineering performance-based tests were conducted to characterize performance of PMAC mixtures. Test protocols and the corresponding engineering properties are listed in Table 5. A brief review of these tests follows.

Table 5

Engineering property tests and protocols

Tests	Protocols	Engineering Properties
Indirect Tensile Strength Test	AASHTO T245	Tensile Properties (fatigue Endurance)
Indirect Tensile Resilient Modulus Test	ASTM D4123	Resilient Modulus (Stiffness)
Indirect Tensile Creep Test	LTRC	Permanent Deformation Characteristics
Frequency Sweep at Constant Height	AASHTO TP7	G*, δ (Viscoelastic Properties)
Repeated Shear at Constant Height	AASHTO TP7	Permanent Strain (Rut Susceptibility)
Simple Shear at Constant Height	AASHTO TP7	Permanent Strain (Rut Susceptibility)
Asphalt Pavement Analyzer Rut Tester	Proposed ASTM	Permanent Deformation (Rut Susceptibility)
Semi-Circular Fracture Test	Mull et al. [19]	Fracture Resistance
Beam Fatigue	SHRP M009	Fatigue Resistance

Indirect Tensile Stress (ITS) and Strain Test. The indirect tensile stress (ITS) and strain test was used to determine the tensile strength and strain of the mixtures. This test was incorporated in the study to ensure that the durability of the mixtures would not be compromised while the rut resistance of the mixtures was being improved. This test was conducted at 25°C in accordance with AASHTO T245. The test specimen was loaded to failure at a 50.8 mm/min (2 in/min) deformation rate. The load and deformations were continuously recorded and indirect tensile strength and strain were computed as follows:

$$S_T = \frac{2 \cdot P_{ult}}{p \cdot t \cdot D}$$

$$e_T = 0.0205\, H_T \qquad (1)$$

where,

S_T – Tensile strength, kPa,

P_{ult} – Peak load, N,

t – Thickness of the sample, mm,

D – Diameter of the specimen, mm,

e_T – Horizontal tensile strain at failure, and

H_T – Horizontal deformation at peak load.

The toughness index (TI), a parameter describing the toughening characteristics in the post-peak region, was also calculated from the indirect tensile test results. A dimensionless indirect tensile toughness index, TI is defined as follows:

$$TI = \frac{A_e - A_p}{e - e_p} \tag{2}$$

where,

TI – Toughness index,

A_e – Area under the normalized stress-strain curve up to strain, e,

A_p – Area under the normalized stress-strain curve up to strain, e_p,

e – Strain at the point of interest, and

e_p – Strain corresponding to the peak stress.

This toughness index compares the performance of a specimen with that of an elastic perfectly plastic reference material, for which the TI remains a constant of one. For an ideal brittle material with no post-peak load carrying capacity, the value of TI equals zero.

Indirect Tensile Resilient Modulus Test. This test is a repeated load indirect tension test for determining the resilient modulus of the asphalt mixtures. The specimens were tested at 5°C, 25°C, and 40°C (40°F, 77°F, and 104°F) in accordance with a modified ASTM D4123 [17]. At these temperatures, 15, 10, and 5 percent of the ITS test failure load were used as the peak values of the cyclic load, respectively. The recoverable vertical deformation, dV, and horizontal deformation, dH, were used to calculate the indirect tensile resilient modulus, M_R and Poisson's ratio, m, according to the following equations:

$$M_R = \frac{P(m + 0.27)}{t \cdot dH(T)}$$

$$m = 3.59\frac{dH(T)}{dV(T)} - 0.27 \tag{3}$$

where,

M_R – Resilient Modulus, MPa,

P – applied vertical load, N,

t – sample thickness, mm,

m - Poisson's ratio,

$dH(T)$ – horizontal deformation at time T, mm, and

$dV(T)$ – vertical deformation at time T, mm.

Indirect Tensile Creep Test. At testing temperatures of 40°C (104°F), a compressive load of 1112.5 N (250 lbf) was applied on the sample using the stress controlled mode of the MTS test system. The load was applied for 60 minutes or until sample failure. The deformations acquired during this time were used to compute the creep modulus as follows:

$$S(T) = \frac{3.59P}{t \cdot dV(T)} \tag{4}$$

where,

$S(T)$ – creep modulus at time T, MPa,
P – applied vertical load, N,
t – sample thickness, mm, and
$dV(T)$ – vertical deformation at time T, mm.

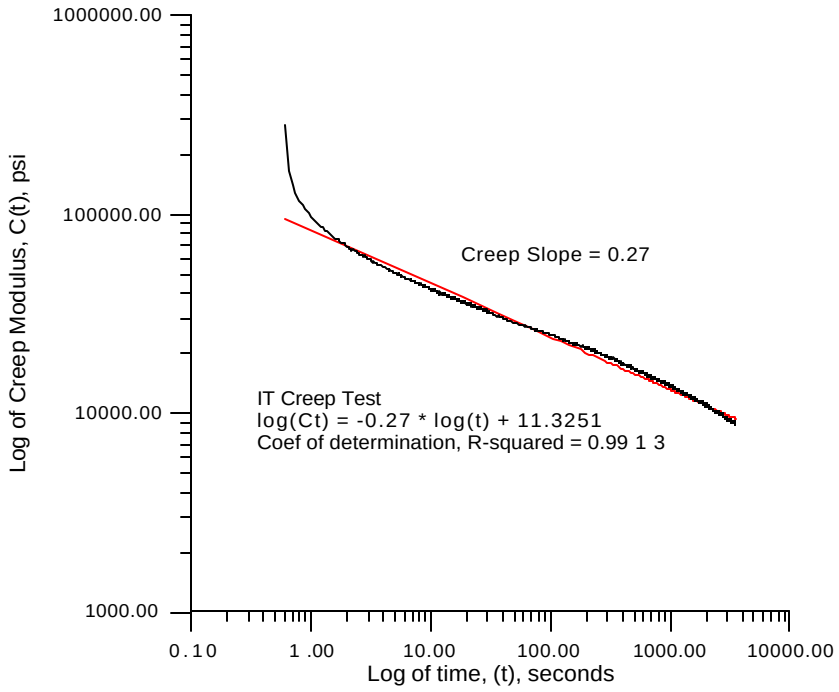

Figure 6
Typical curve of indirect tensile creep modulus vs. time

Figure 6 shows a typical creep modulus versus time graph on a log-log scale for the indirect tensile creep data. The creep slope was computed from this graph and used in the analysis. Higher stiffness, lower creep slope and lower permanent strain are desired for rut-resistant mixtures. Texas specifications specify a minimum stiffness of 41.4 MPa, maximum creep

slope of $3.5x10^{-8}$, and maximum permanent strain value of $5x10^{-4}$ mm/mm for a satisfactory surface mixture [18].

Frequency Sweep at Constant Height (FSCH) Test. The Superpave simple shear frequency sweep at constant height (FSCH) test, conducted in the shear mode, is a strain controlled test in which a specific amount of deformation is induced in the specimen. Stress generated in the specimen is not controlled but is simply the reaction to the induced strain. The sinusoidal shear strain with peak amplitude of approximately 0.05μm/mm is applied at frequencies of 10, 5, 2, 1, 0.5, 0.2, 0.1, 0.05, 0.02 and 0.01 Hz. This strain level was selected during the SHRP Program to ensure that the viscoelastic response of the asphalt mixture is within the linear range. This means that the ratio of stress to strain is a function of loading time (or frequency) and not of the stress magnitude. An axial stress is applied to maintain constant height. A Superpave shear tester was used in this study with a test temperature of 60°C. Frequency is directly related to traffic speed. Hence, the frequency sweep test can be used to evaluate the performance of an asphalt mixture at different traffic speeds.

Repeated Shear at Constant Height. This is a stress-controlled test. A repetitive shear load (haversine) is applied to the specimen to generate a shear deformation. The shear load is applied with a maximum shear stress of 68 kPa for a loading time of 0.1 sec and a rest period of 0.6 sec. Then, repetitive loading is applied for a total of 5,000 repetitions or until five percent shear strain is reached. An axial stress is applied to maintain constant height.

While developing the repeated shear test at constant height, two mechanisms that provide resistance to permanent deformation in an asphalt mixture were hypothesized:

- Asphalt Binder Stiffness - Stiffer binders help in resisting permanent deformation as the magnitude of the shear strains is reduced under each load application. The rate of accumulation of permanent deformation is strongly related to the magnitude of the shear strains. Therefore, stiffer asphalt will improve rutting resistance as it minimizes shear strains in the aggregate skeleton.
- Aggregate Structure Stability - The axial stresses act as a confining pressure and tend to stabilize the mixture. A well-compacted mixture will develop high axial forces at very small shear strain levels. Poorly compacted mixtures can also generate similar levels of axial stresses, but they will require much higher shear strain.

Simple Shear at Constant Height

As described in test procedure G of the AASHTO TP7 [9], the simple shear at constant height (SSCH) test is a controlled stress test that applies an increasing shear stress to a cylindrical test specimen until a specified shear stress level (35 kPa) is achieved. The

specified shear stress is held constant for 10 seconds and then released (unloading) at a specific rate. The unloading period will last for 15 seconds to let the shear strain relax. During the test, a varying axial stress is applied automatically to maintain a constant height for the specimen. The primary response variable from this test is the maximum permanent shear strain at the end of testing. In this test, the two mechanisms are free to fully develop their relative contribution to the resistance of permanent deformation as they are not constrained by imposed axial or confining stresses.

APA Rut Test. The Asphalt Pavement Analyzer (APA) is the new generation of the Georgia Loaded Wheel Tester (GLWT). The APA can test three beam samples (330 x 120 x 75 mm) or six cylindrical samples (150 mm x 76 mm) simultaneously. The concave shaped wheels travel back and forth over a stiff, pressurized rubber hose that rests directly on the specimen. Typical test conditions as set by the Georgia Department of Transportation specification are only for beam specimens. The Georgia specification sets a test temperature of 40°C, vertical load of 444.4 N, and 0.7 MPa hose pressure with the criteria of no more than 7.6 mm rut depth after 8,000 cycles (16,000 passes) under dry conditions. The wheel speed is approximately 60 cm/sec.

In this study, beams were tested at 64°C because of the binder type selected. Vertical load, hose pressure, and wheel speed were the same as those specified in Georgia specification. An automated system that continuously measures the rut depth was adopted. Figure 7-1 shows a typical APA rut test curve. Rut depths at 8,000 cycles were recorded for analysis.

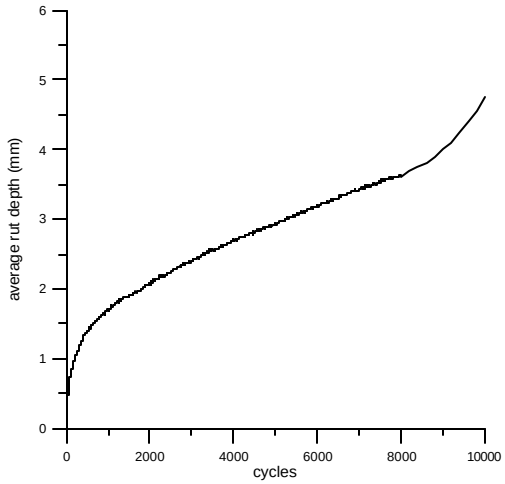

Figure 7-1
APA rut depth vs. load cycles

Semi-Circular Fracture Test. The semi-circular fracture test, first introduced to characterize the fracture resistance of crumb rubber modified asphalt mixtures [19], is based on a fracture mechanics concept - the critical strain energy release rate, also called the critical value of J-integral, or Jc. In this study, the fracture resistance of Superpave mixtures with various percentages of RPMAC contents was characterized using this test based on notched semi-circular specimens [20]. Figure 7-2 shows the semi-circular test setup used at LTRC and the corresponding dimensions [20]. During the test, the specimen was loaded monotonically to failure at a constant cross-head deformation rate of 0.5 mm/min in a three-point bend load configuration, as shown in Figure 7-2. The load and deformation were continuously recorded and the critical value of J-integral (J_c) was determined as follows:

$$J_c = -\left(\frac{1}{b}\right)\frac{dU}{da}$$

Where: *b* is sample thickness, *a* is the notch depth and *U* is the strain energy to failure.

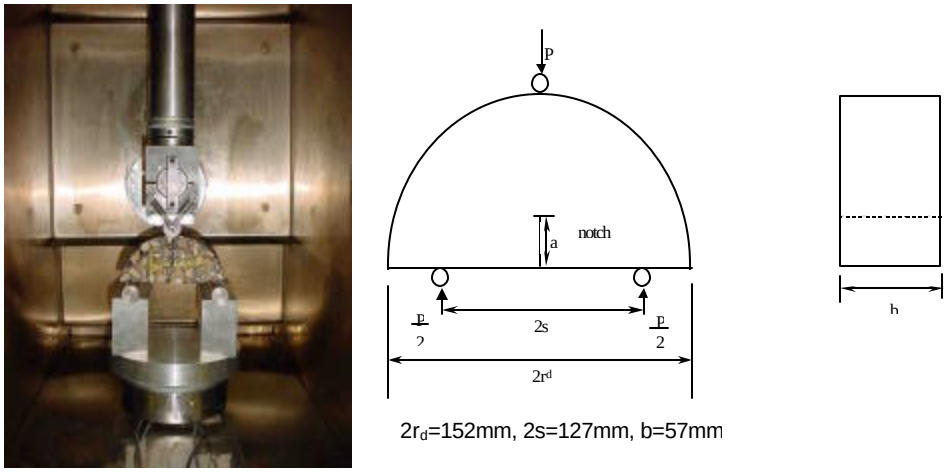

Figure 7-2
LTRC Set-up of Semi-Circular Fracture Test

To determine the critical value of J-integral, semi-circular specimens with at least two different notch depths (parameter "a" in Figure 7-2) need to be tested for one mixture. In this study, three notch depths of 25.4 mm, 31.8 mm, and 38 mm were selected based on an a/r_d ratio (the notch depth to the radius of the specimen) of between 0.5 and 0.75 [20, 21]. For each notch depth three duplicates were tested. The test temperature was 25 ^oC. According to the test protocol, four semi-circular specimens with a dimension of 150mm by 57mm can be cut from one single SGC 150mm-sample.

Beam Fatigue Test. This test is conducted according to SHRP M009 protocol at 25ºC (77ºF). It is a strain-controlled test in which a beam 318 mm (15 in) long by 63.5 mm (2.5

in) wide by 50.8 mm (2.0 in) high is subjected to 4-point bending. The strain level selected will be such that failure does not occur prior to 10,000 cycles. The center deflection of the beam is continuously measured and used in the computation of the stiffness. Failure is defined as the load cycle at which the specimen exhibits a 50 percent reduction in stiffness. The number of cycles to failure (N_f) was used in the analyses. The reported test results were the average of two test samples.

Specimen Preparation

This research mainly deals with the recycled PMAC (binder). Therefore, the only variable in this study was asphalt binder. Basically, lab-aged and field-aged asphalt binder was provided by the Chemistry Department at Louisiana State University, and the lab personnel mixed the virgin binder with the aged one according to the required percentage (20, 40 and 60 percent). No aged or recycled aggregates were considered in this study. The mixed binder and the virgin aggregate (Limestone) were used in the mixture design. Four sizes of specimens were fabricated for mixture fundamental engineering property tests in this study, including two sizes of cylindrical specimens and two sizes of beam specimens.

The 100mm (4 in) diameter by 63.5mm (2.5 in) high cylindrical specimens were compacted with the Superpave Gyratory Compactor (SGC) for the indirect tensile resilient modulus, creep and axial creep tests. The target air void for the mixtures was 4 ± 0.5 percent.

The 150mm diameter cylindrical specimens were compacted with the SGC in accordance with AASHTO Designation TP4 for the Superpave Shear Tests. The N_{design} used was 125 SGC gyrations. Each compacted specimen, which was 150mm in diameter and approximately 130 to 140 mm high, was cut into two test specimens. These test specimens met the AASHTO TP7 height requirements of 50 ± 2.5 mm for performance based testing.

The Semi-circular fracture test specimens in this study were also obtained from the 150mm SGC compacted cylindrical specimens. Each SGC cylindrical specimen was compacted at an air void content of 7.0 ± 0.5 percent with a dimension of 150mm in diameter and 57mm in height. Two SCB test specimens were then cut from one SGC core along the central axis. A vertical notch was then introduced along the symmetrical axis of each SCB specimen. The notches were cut using a special saw blade of 3.0 mm thickness. Three nominal notch depths of 25.4 mm, 31.8 mm and 38 mm were used. For each notch depth, three duplicate SCB specimens were prepared.

The APA beam specimens [330mm (13 in) long by 120mm (5 in) wide and 75mm (3 in) high] were compacted using a vibratory kneading compactor at a target air void of 4.0 ± 0.5 percent. The beam fatigue specimens [381 mm (15 in) long by 63.5 mm (2.5 in) wide by 50.8 mm (2.0 in) high] were also compacted using a vibratory kneading compactor with the target air void of 4.0 ± 0.5 percent.

DISCUSSION OF RESULTS

Binder Rheological Properties

Original (Tank) PMAC Binder

The PAC-40HG sample was subjected to standard short-term and long-term aging procedures and then characterized according to the SHRP protocol. The results are presented in Tables 6 and 7. The data were consistent with that reported by the industrial provider of asphalt samples.

Table 6
Original AC-30 binder rheological characterization

Material			AC-30
Weight Loss, %	After TFOT		<1%
BBR, after PAV, -16°C	Stiffness (MPa)		173
	Slope (m)		0.348
DSR test	G*/sinδ @64°C, pa	Original	1448
		TFOT	4295
		PAV	12893
	G*/sinδ @76°C, pa	Original	338
		TFOT	832
		PAV	2491
	G*/sinδ =1000pa@T°C	Original	66.8
		TFOT	72.2
		PAV	83.1

Table 7
Rigidity test results

Parameter	AC-30	PAC-40HG
	Original	
1. Work, Nm (lbm)	0.04 (0.48)	18.65 (165.35)
2. Maximum load, N (lb)(F_2)	70.02 (15.77)	134.58 (30.31)
3. Load at 100% elongation, N (lb)(F_1)	-	61.01 (13.74)
4. Elongation at maximum load, m (in)	0.0025 (0.0984)	0.0123 (0.484)
5. F_1/F_2		0.45
	TFOT Aged	
6. Work, Nm (lbm)	11.2 (99.28)	15.56 (146.86)
7. Maximum load, N (lb)(F_2)	163.17 (36.75)	134.27 (30.24)
8. Load at 100% elongation, N (lb)(F_1)	-	53.32 (12.01)
9. Elongation at maximum load, m (in)	0.008 (0.315)	0.0085 (0.3346)
10. F_1/F_2	-	0.40
	PAV Aged	
11. Work, Nm (lbm)	0.16 (1.4)	15.36 (136.24)
12. Maximum load, N (lb)(F_2)	103.76 (23.37)	127.83 (28.79)
13. Load at 100% elongation, N (lb)(F_1)	-	52.35 (11.79)
14. Elongation at maximum load, m (in)	0.0027 (0.1063)	0.0112 (0.4396)
15. F_1/F_2	-	0.41

PMAC and Aged PMAC Blends

The feasibility of using recycled PMAC was studied by blending the virgin PMAC with lab-aged (PAV-aged) PMAC at different percentages (0, 20, 40, 60 percent) at 100 to 135°C. The lab-aged PMAC was consistently stiffer than the virgin asphalt, as would be expected from extended field aging. The relative stiffness of the blends, expressed as $G^*/\sin\delta$ at selected qualification temperatures is summarized in Table 8. Based on the specification of a minimum $G^*/\sin\delta$ = 1000 Pa, the addition of aged PMAC raised the minimum temperature for qualification with regards to stiffness.

Table 8
Rheological data for blends of PMAC with PAV-aged PMAC

Material (% PAV PMAC)	G*/sinδ@64°C Pa	G*/sinδ@76°C Pa	G*/sinδ = 1,000Pa@T°C
0%	3,615	1,029	76.1
20%	4,400	1,244	78.4
40%	5,250	1,488	79.9
60%	8,263	2,148	82.8
100%	18,927	5,135	92.8

The consistency of the blends was measured by rotational viscosity at 135°C. Although an increase in viscosity was noted (Table 9), neither the blends nor the pure PAV aged PMAC exceeded the practical limit of 3.0 Pa.s for high temperature viscosity. The presence of the polymer additive exerted a moderating influence on the age hardening of the asphalt matrix. Therefore, the preliminary results indicate that recycling of PMACs should be feasible.

Table 9
Viscosity of blends of PMAC with PAV-aged PMAC

Material (% PAV-aged PMAC)	Viscosity @ 135°C (Pa.s)
0%	1.125
20%	1.340
40%	1.547
60%	1.832
100%	2.580

All blends were PAV-aged, and their stiffness was determined by measuring the low-temperature creep response using a Cannon bending beam rheometer (BBR). The Superpave SHRP protocol was observed for these measurements. The data, which were collected at six loading times (8, 15, 30, 60, 120, and 240 sec) for a load on the beam of 100 ± 5 g, allowed the calculation of the creep stiffness, *S(t)*, and the creep rate of the sample under load, *m*, as the absolute value of the slope of the log stiffness versus log time curve. The results are shown in Figure 8. As expected, the stiffness increased with the content of the aged material; however, it remained in the lower half of the accepted maximum value. Accordingly, the creep rate experienced a low decrease, remaining much above the minimum qualifying value.

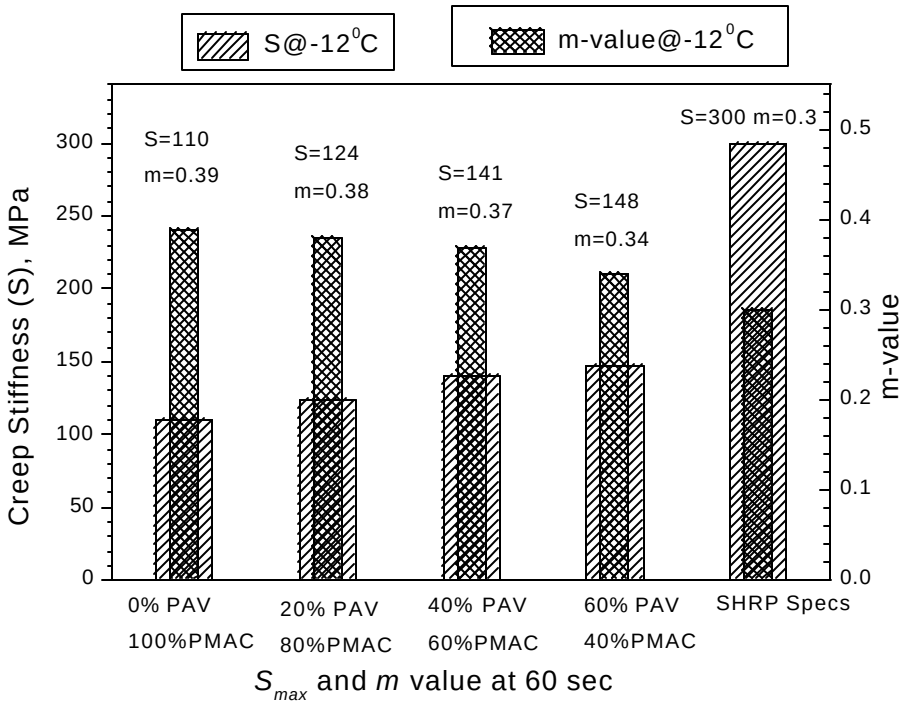

Figure 8

Creep and creep stiffness determined at -12° C for PAV-aged PMAC blends containing *a priori* PAV-aged PMAC material

PMAC and Field-Aged PMAC Blends

To establish the feasibility of blending recycled US61 binder with virgin PMAC, blends of PMAC with various percentages of US61 binder were made at 100 to 135°C. Table 10 presents the test results of binder rheology at selected qualification temperatures. As seen in Table 10, the US61 binder was consistently stiffer than the virgin asphalt, as would be expected from extended field aging. In addition, the high temperature stiffness factor, or the rutting factor of the blends, expressed as G*/sinδ at selected high temperatures, increased significantly after the addition of only 20 percent US61 binder to the PMAC: the G*/sinδ value jumped from 1.03 kPa to 23.8 kPa. The higher the G*/sinδ value, the better the binder resisted permanent deformation. On the other hand, the fatigue cracking factor, termed as G*sinδ at intermediate temperatures, also increased rapidly because of the inclusion of the US61 binder. It is noted that all the G*sinδ values of various of US61 binder contents (20, 40 and 60 percent) at 25°C exceeded the maximum Superpave specification value of 5,000 kPa, indicating high fatigue cracking tendency for the binders. Moreover, BBR test results showed that the addition of US61 binder also increased the thermal cracking potential.

Table 10
Rheological data for blends of PMAC with US-61S

Test	Property	Test Results				PG Criteria
		0% US-61S	20% US-61S	40% US-61S	60% US-61S	
Original Binder						
Dynamic Shear Rheometry (kPa)	**G*/sin** d	@ 70°C 1.782 @ 76°C 1.029 @ 82°C 0.55	@ 70°C 42.3 @ 76°C 23.8 @ 82°C 13.6	@ 70°C 160 @ 76°C 94.8 @ 82°C 54.4	@ 70°C 187 @ 76°C 99.7 @ 82°C 53.4	1.0 kPa, Min
PAV Aged Binder						
Dynamic Shear Rheometry (kPa)	**G*sin** d	@28°C 1036.3 @ 31°C 707.4	@25°C 5229.5 @28°C 3716.5 @ 31°C 2657.5	@25°C 6911.3 @28°C 5360.9 @ 31°C 3917.2	@25°C 8889.1 @28°C 7064.9 @ 31°C 5518.8	5000 kPa, Max.
Bending Beam Rheometry (-12°C)	Stiffness	110	219	246	249	300 MPa, Max.
Bending Beam Rheometry (-12°C)	M value	0.39	0.271	0.246	0.229	0.300, Min.

Binder Extraction and Recovery

As mentioned before, two techniques were developed and used in this study to extract and recover the binder from RPMAC mixtures. A supercritical extraction procedure, SCF, was compared with a toluene extraction procedure.

The rheological properties of the PMAC sample extracted under SCF conditions were compared to those of the original sample to check if the extraction process altered the

material properties. As shown in Figure 2, the rheology of the extracted sample compared very well with that of the original PMAC over the whole range of temperature.

A Bohlin CVO dynamic shear rheometer (DSR) specially designed to characterize asphalt cements (Bohlin Instruments Div., Metric Group Inc., Cranbury, New Jersey) was used to investigate the rheological behavior of the extracted binder. The SHRP protocol was employed for performing the measurements. The DSR results for binders extracted from an aged mixture containing PAC-40, PAV-aged PMAC, and virgin binder (viz., the reference material for the mixtures containing blends of aged and non-aged PAC-40) are shown in Figure 9.

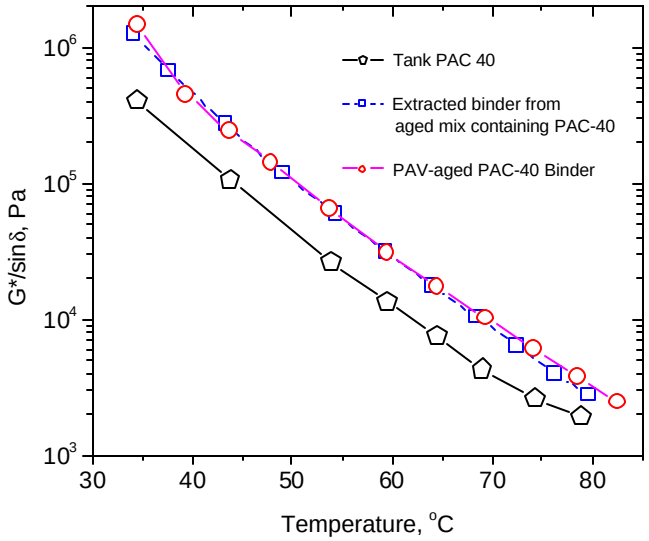

Figure 9
Temperature / stiffness relationship of different binders

Figure 9 demonstrates that the stiffness of the extracted binder, as expressed by the SHRP G*/sinδ parameter, was above the stiffness of the PAC-40 and well above the minimum requirement of 1,000 Pa for temperatures up to 90°C. At the same time, there was practically no difference between the stiffness of the binder that was PAV-aged while in the mix and subsequently extracted and the stiffness of the PAV-aged PAC-40 binder. However, when one compares the value of sinδ at higher temperatures (Figure 10), one may observe that the elastic character of the binder, reflected by sinδ <1.0, is enhanced after aging. Table 11 lists the storage modulus G' at 80°C. As expected, the elasticity of the binding system was enhanced by aging, perhaps because aging created a more compatible network system.

Therefore, blending with virgin asphalt cement will yield PAC-40 type binders with qualifying stiffness values for a rather large range of high temperatures.

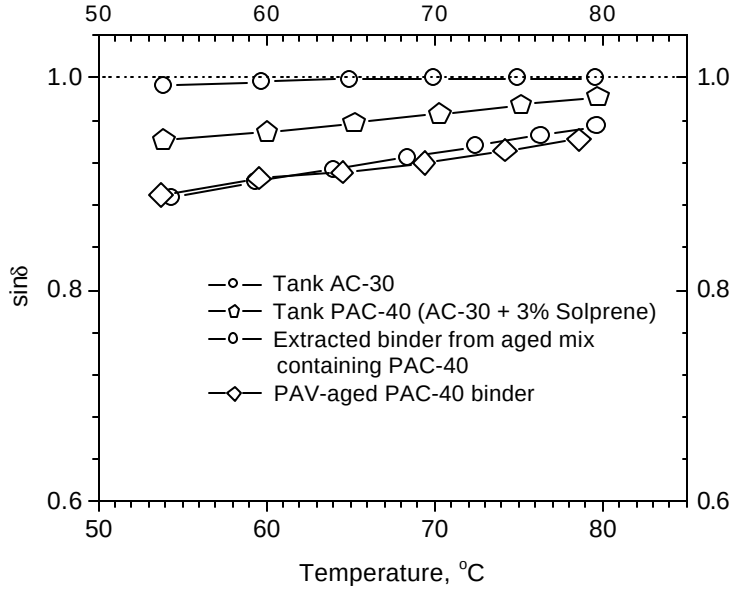

Figure 10

Variation of sind **with temperature of the AC-30, PAC-40, PAV-aged PAC-40 and the binder extracted from the long-term aged mix containing PAC-40**

Table 11

Elastic character of binders at high temperatures as reflected by the value of the storage modulus G' = G* cosd **at 80° C**

Binder	d **(°)**	**G'**
AC-30	90	0
PAC-40	79.02	0.19G*
PAV-Aged PAC-40	72.50	0.30G*
Extracted Mix-Aged PAC-40	71.26	0.32G*

Fractionation of PMAC Binder

The polymer was separated from the PAC-40HG by dissolving the sample in toluene and then fractionally precipitating the polymer by adding a methanol/toluene mixture (2:1 vol:vol) to the solution. To confirm that the fractionation process did not affect the

properties of the sample, PAC-40HG was dissolved in toluene and then recovered. The rheological properties of the recovered sample were essentially identical to those of the material.

Characterization of Binder by Chemical Analysis

FTIR. The composition of the PMAC was studied using infrared (IR) spectroscopy. In the infrared region, the frequency of electromagnetic radiation corresponded to the vibrational frequencies of molecules. Hence, the absorbance of IR radiation was due to the bending and stretching motions of the molecules. Molecular vibrations give rise to IR bands only if they cause a change in the dipole moment of the molecule. If a stretch does not change the dipole moment, there will not be any IR band. This is why O_2 and N_2 in the atmosphere do not show any IR bands. Carbon dioxide, CO_2, however, has a stretch where one O moves in and the other moves out:

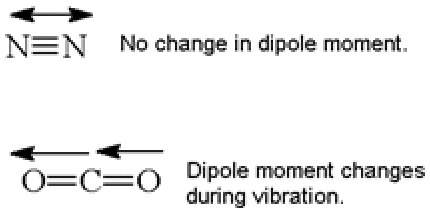

A typical IR spectrum will have absorbance bands that can be attributed to the presence of individual chemical groups in the molecule under study and a "fingerprint" region distinctive of the individual compound.

A Fourier Transform Infrared (FTIR) spectrometer uses the technique of Michelson interferometry. A beam of radiation from the source, S, is focused on a beam splitter constructed so that half the beam is reflected to a fixed mirror. The other half of the beam is transmitted to a moving mirror that reflects the beam back to the beam splitter from where it travels, recombined with the original half beam, to the detector, D (Figure 11).

The recombined beam passes through the sample before hitting the detector. The sample absorbs all the different wavelengths characteristic of its spectrum, and this subtracts specific wavelengths from the interferogram. The detector now reports variation in energy versus time for all wavelengths simultaneously. Energy versus time is an odd way to record a spectrum. Because *time* and *frequency* are reciprocals, a mathematical Fourier transform function allows the conversion of an intensity-vs.-time spectrum into an intensity-vs.-frequency spectrum. The IR intensity variation with optical path difference (interferogram) is the Fourier transform of the (broadband) incident radiation. A laser beam is superimposed to

provide a reference for the instrument operation. The IR absorption spectrum can be obtained by measuring an interferogram with and without a sample in the beam and transforming the interferograms into spectra.

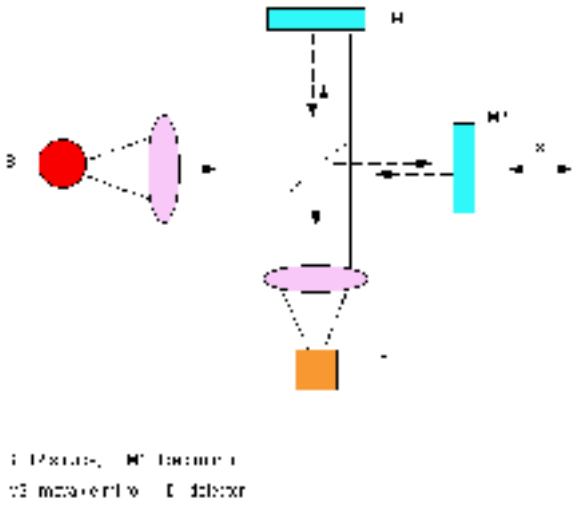

Figure 11
Principle of an FTIR instrument

Most spectra using electromagnetic radiation are presented with the wavelength as the X-axis. Originally, IR spectra are presented in units of micrometers. However, a linear axis in micrometers compresses the region of the spectrum (10-15 µm) that usually has the largest number of peaks. Therefore, a different measure, the wave number (n), is derived as follows: n **(cm $^{-1}$) = 10,000/**l **(**m**m).** On the wave number scale (4,000-400 cm^{-1}) the vibration of carbon dioxide, O=C=O, is seen as a band at 2,400 cm^{-1}. The C-H from C single bonds appears at around 2,800-3,000 cm^{-1} and the non-aromatic C=C double bonds absorb in the 900-1,000 cm^{-1} region. The carbonyl C=O double bonds, of particular interest for the analysis of asphalt oxidation, appear in the region of 1,650-1,800 cm^{-1}, with specific bands for acids (1,650-1,700 cm^{-1}), esters (1,740-1,750 cm^{-1}), aldehydes (1,720-1,750 cm^{-1}) and ketones (1,720-1,750 cm^{-1}). Also, aromatic rings show "overtones" centered at around 1600 cm^{-1}.

The major bands in the parent AC-30 (Figure 12A) were identified as typical hydrocarbon absorbancies at 2,952; 2,923; and 2,852 cm^{-1}. Weaker bands were noted at 1,453 and 1,377 cm^{-1}. The polymer additive, an SBS rubber, exhibited a similar set of hydrocarbon bands (Figure 12B); however, one unique band at 966-968 cm^{-1}, corresponding to residual unsaturation, was noted. Using this band it was possible to detect the presence of the polymer in the PMAC (Figure 12C). To confirm that this band was indeed characteristic of

the polymer, additional quantities of polymer were added to PMAC, and a corresponding increase in the band intensity at 966 cm^{-1} was observed (Figure 12D).

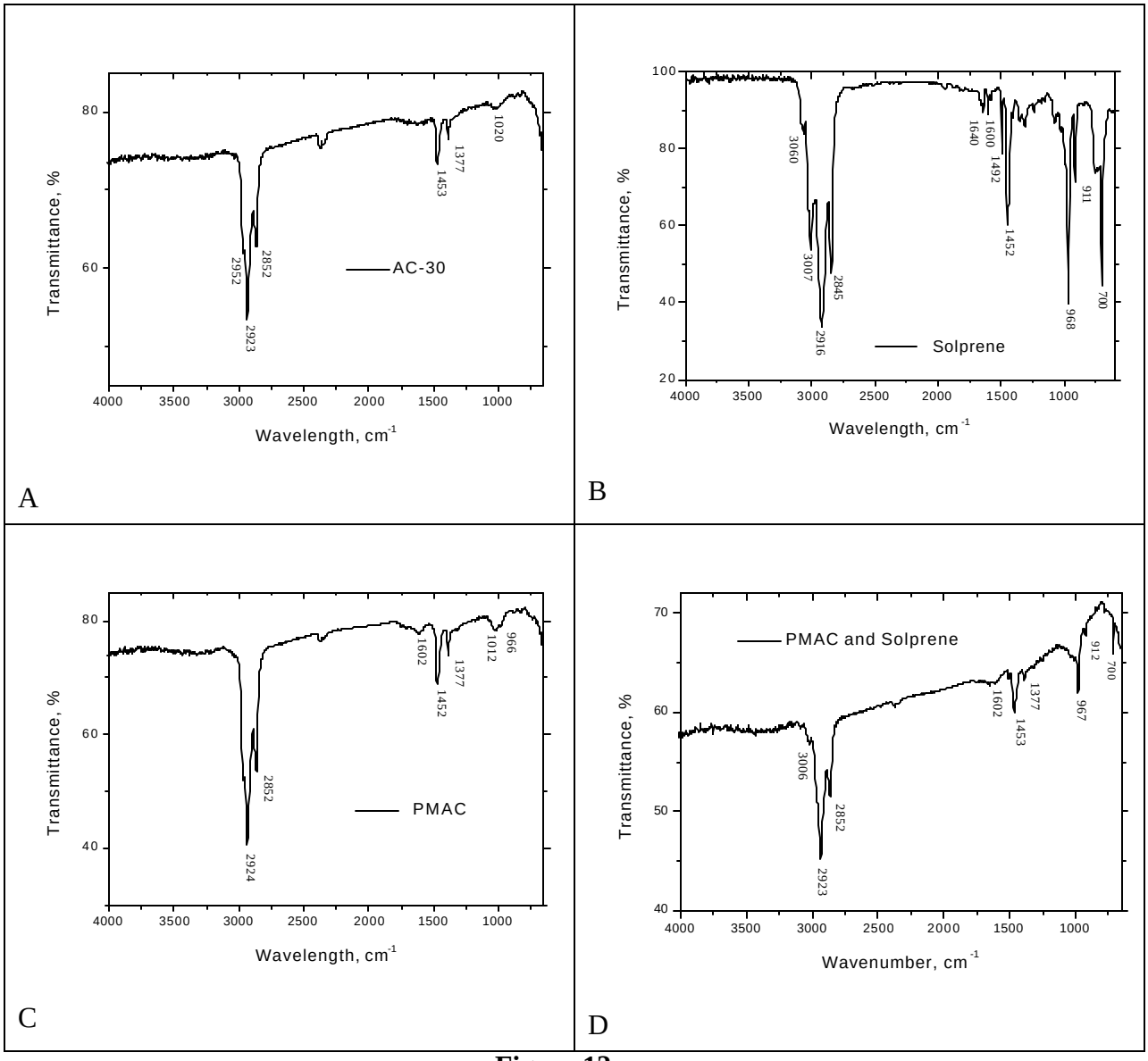

Figure 12

FTIR spectra of PMAC components and of polymer spiked PMAC (film on NaCl plate)

Aging is reflected in the infrared spectra of asphalts by multiple peaks centered around 1,698 cm^{-1}, which corresponded to carbonyl (C = O) absorptions of oxidized species, such as ketones or carboxylic acids [5, 18]. By comparing the intensity of the 1,698 cm^{-1} region to that of 1,600 cm^{-1}, which is attributed to aromatic ring vibrations, the relative degree of oxidation of the samples can be estimated. The more oxidized the asphalt (e.g., PAV-aged), the more intense the 1,698 cm^{-1} peak becomes and the corresponding 1,698/1,600 cm^{-1} ratio increases. Figure 13 presents the FTIR spectra of the original and of the thin film oven test

(TFOT) and PAV- aged AC-30 samples. Carbonyl species are present also in the asphalt, but their concentration increases with the extent of aging, i.e., TFOT or PAV air oxidation. The 1,698/1,600 cm^{-1} ratio calculated from the spectrum is not relevant for virgin and TFOT-aged asphalts (no workable bands are present in this region in their FTIR spectra due to the lack of oxidized species). After PAV aging, the sample was clearly oxidized; the 1,698/1,600 cm^{-1} ratio was 0.53. A similar trend was observed in the spectra of PMAC and field aged materials (Figures 14 and 15). In the PMAC spectra, oxidation of the sample is clearly identified already in the TFOT aged PMAC sample; the ratio increases from 0.50 to 0.55 and continues to increase in the sample subjected to PAV (0.77). The higher auto-oxidative sensitivity of PMAC suggests that the polymer additive is behaving as a sacrificial antioxidant. The allylic positions adjacent to the C = C double bonds within polybutadiene blocks can readily react with oxygen, particularly at elevated temperatures (t >100°C), bringing about a significant increase of carbonyl species and a concomitant cleavage of the polymer backbone. The reduction in molecular weight can be detected using gel permeation chromatography (*vide infra*).

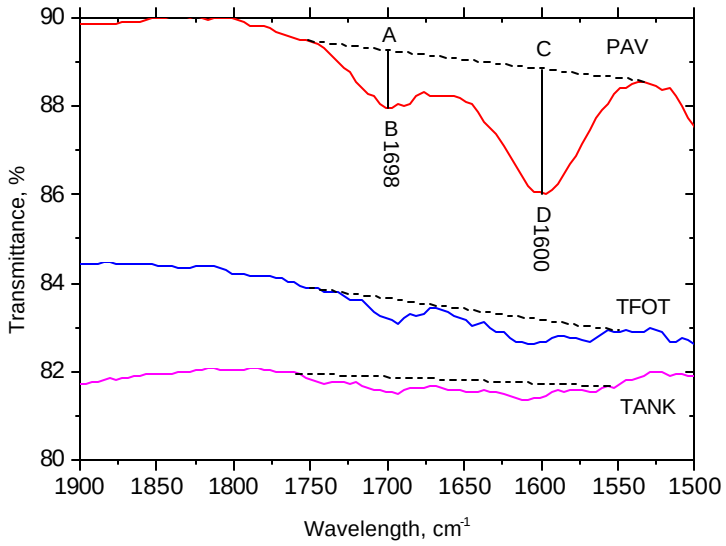

Figure 13
Comparative FTIR spectra of the original and aged AC-30 asphalt samples (films on NaCl plates)

Thermo-oxidative degradation of SBS elastomers occurs within the polybutadiene segment only; no oxidation of the polystyrene segments is expected [22]. After extensive oxidation, the polymer is effectively degraded and can no longer be detected in the aged binder. Although oxidation of the asphalt components may be retarded by the presence of the

polymer, age hardening continues to occur [5]. The field aged binder exhibits a higher extent of oxidation than the PAV aged PMAC; the 1,698/1,600 ratio is A:B = 1.76. Dilution with virgin PMAC effectively reduced the concentration of aged material; the 1,698/1,600 ratio decreased to 1.58, 1.33 and 0.96 for samples containing 60, 40, and 20 percent, respectively (Figure 15).

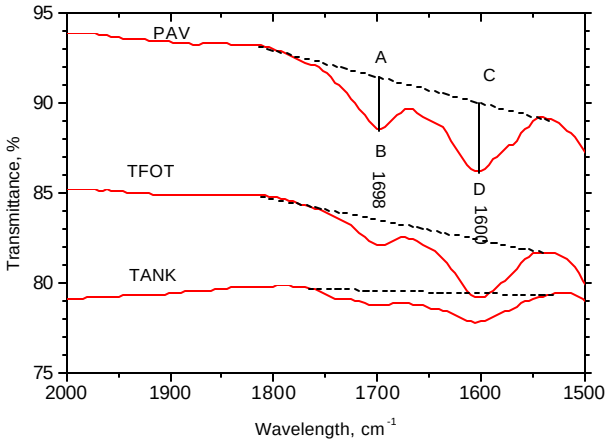

Figure 14
Comparative FTIR spectra of the original and aged PMAC samples (on NaCl plates)

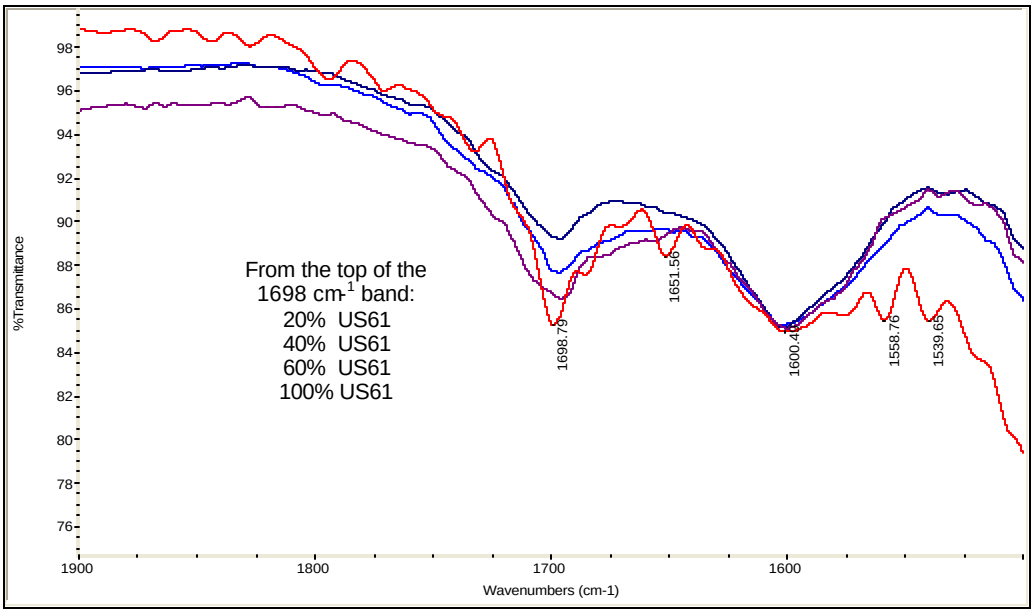

Figure 15
Comparative FTIR spectra of blends made with PMAC containing 20, 40, and 60 percent US61 binder (films on NaCl plates)

Gel Permeation Chromatography. Size-exclusion chromatography (SEC), also called gel-filtration or gel-permeation chromatography (GPC), uses porous particles to separate molecules of different sizes. It is generally used to separate and to determine molecular weights and molecular weight distributions of polymers. A mechanical pump ***B*** (Figure 16) provides an eluting solvent from reservoir ***A*** to push the sample along in columns ***D***.

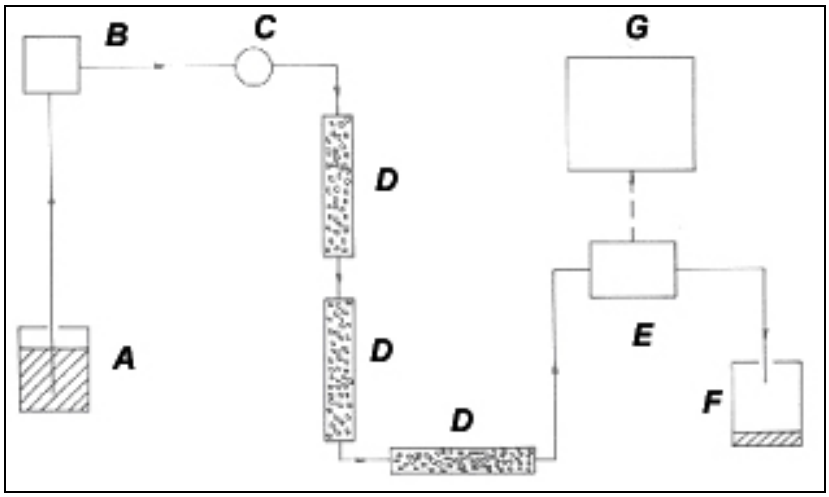

Figure 16

Schematic illustration of a GPC apparatus: *A*, solvent reservoir; *B*, solvent pump; *C*, injection valve; *D*, GPC column; *E*, detector; F**, waste solvent/solution reservoir; and *G*, computer**

The individual molecules diffuse through the column volume, and sometimes enter the pores of the column packing material (a gel, Figure 17).

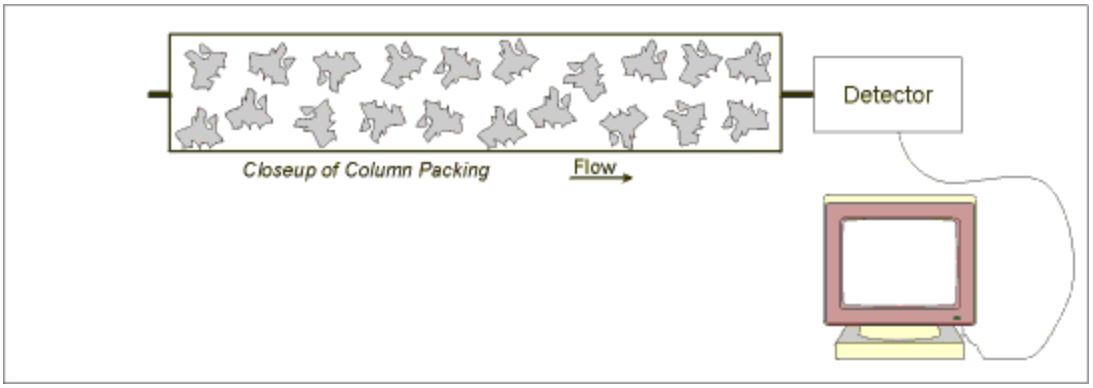

Figure 17

Close-up of a column packing showing the pores

The columns are designed so that the larger molecules do not fit into many of the pores (they are excluded), so they run through the column quickly (Figure 18).

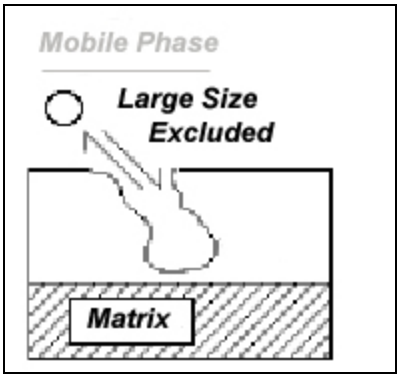

Figure 18
Principle of GPC: Larger size molecules excluded from pores

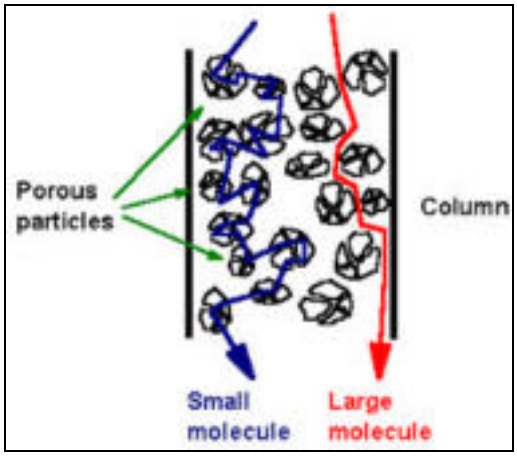

Figure 19
Schematic of a size-exclusion chromatography (GPC) column.

On the other hand, the smaller molecules in the sample can fit into most of the pores, occasionally getting stuck there, so they diffuse along more slowly. Because molecules that are smaller than the pore size can enter the particles, they have a longer path and longer transit time than larger molecules that cannot enter the particles (Figures 19 and 20). This setup leads to the counter-intuitive result that the biggest molecules come out first, and the smallest ones last. SEC essentially sorts the molecules based on their average size in solution ("hydrodynamic volume").

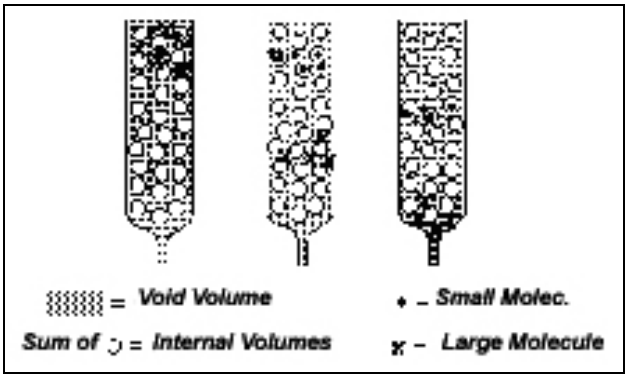

Figure 20

Depiction of transit pathways of various sized molecules

Molecules larger than the pore size can not enter the pores and elute together as the first peak in the chromatogram (Figure 21). This condition is called total exclusion. Molecules that can enter the pores will have an average particle residence time that depends on the molecule's size and shape. Different molecules, therefore, have different total transit times through the column. This portion of a chromatogram is called the selective permeation region. Molecules that are smaller than the pore size can enter all pores, and they have the longest residence time on the column and elute together as the last peak in the chromatogram. This last peak in the chromatogram determines the total permeation limit.

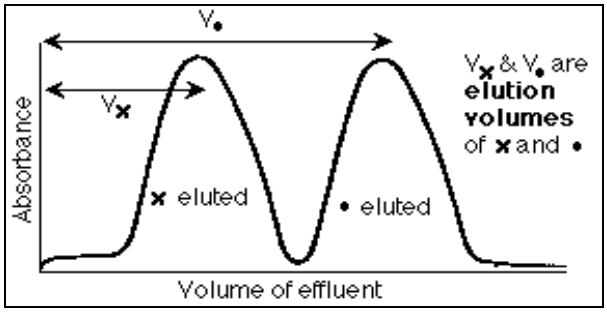

Figure 21

Building of a GPC chromatogram based on elution volume (time).

To determine the molecular mass of polymers, a calibration of columns with similar polymeric species of known molecular mass is needed (Figure 22).

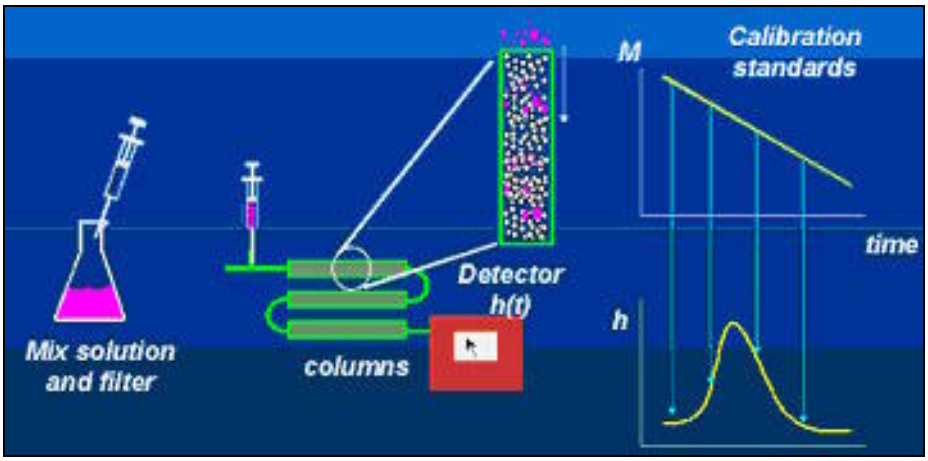

Figure 22
General scheme for a GPC experiment

Experimentally, a GPC analysis for determination of molecular mass of polymers starts with the preparation and filtration of a dilute polymer solution (e.g., 0.25 percent). The solution is then injected into the column at the time t = 0 min and some characteristics of the eluate from the columns, such as absorption of UV light or the refractive index, are compared in the detector to the characteristics of the pure solvent. The peak height (h) is related to the polymer sample concentration of molecular species of mass (M), as determined from the calibration curve (Figure 22).

Dilute polymer solutions (c<0.5 percent) should be analyzed by GPC because the polymer molecules are not entangled (Figure 23) in dilute solutions, and they can be separated as individual species.

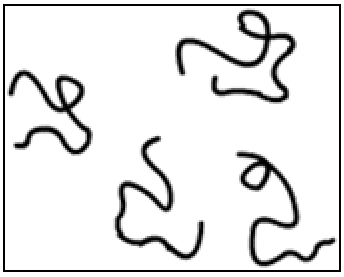

Figure 23

Individual polymer molecules in diluted solutions

In more concentrated solutions, the macromolecules can entangle and form aggregates stabilized by secondary forces (such as hydrogen bonding or p-p interactions between aromatic nuclei), as depicted in Figure 24.

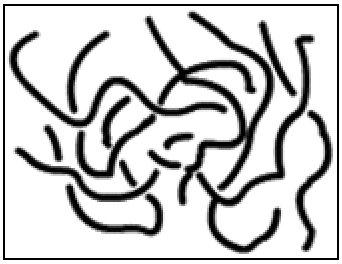

Figure 24
Aggregated polymer molecules formed in concentrated solutions

Such aggregates can appear larger than the pore size and will be excluded, giving an erroneous indication of very high molecular mass for the analyzed polymer. If the polymer molecules are linked through stable chemical bonds, e.g., covalently bonded, insoluble crosslinked "aggregates" will form. Even for a very high solvent:polymer ratio (e.g., > 1,000), the crosslinked polymer (Figure 25) does not dissolve and forms gels by absorbing the solvent. Insoluble polymeric species and gels are precluded from entering the columns through filtration by a short guard column.

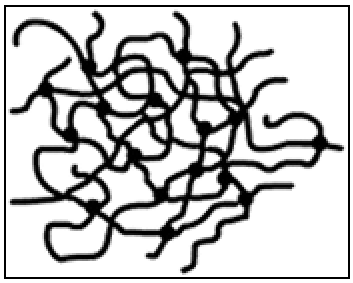

Figure 25

Crosslinked polymer molecules

The polymer and asphalt components of PMAC could be separated using gel permeation chromatography (GPC). Solutions of the asphalt samples were prepared in tetrahydrofuran (THF) and analyzed. The parent AC-30 eluted in a relatively broad band centering at an elution volume of 27.9 mL or at a molecular weight of ~1,000 Daltons (Figure 26A). The SBS sample eluted at 20.95 mL (Figure 26B), which corresponds to a molecular weight of 110,000 Daltons. The large differences in the molecular weights between the asphalt and polymer components allowed baseline separation of the two components in the GPC chromatogram of a prepared mixture containing approximately 15 percent SBS (Figure 26C). When the technique was applied to the PMAC sample, the SBS component was

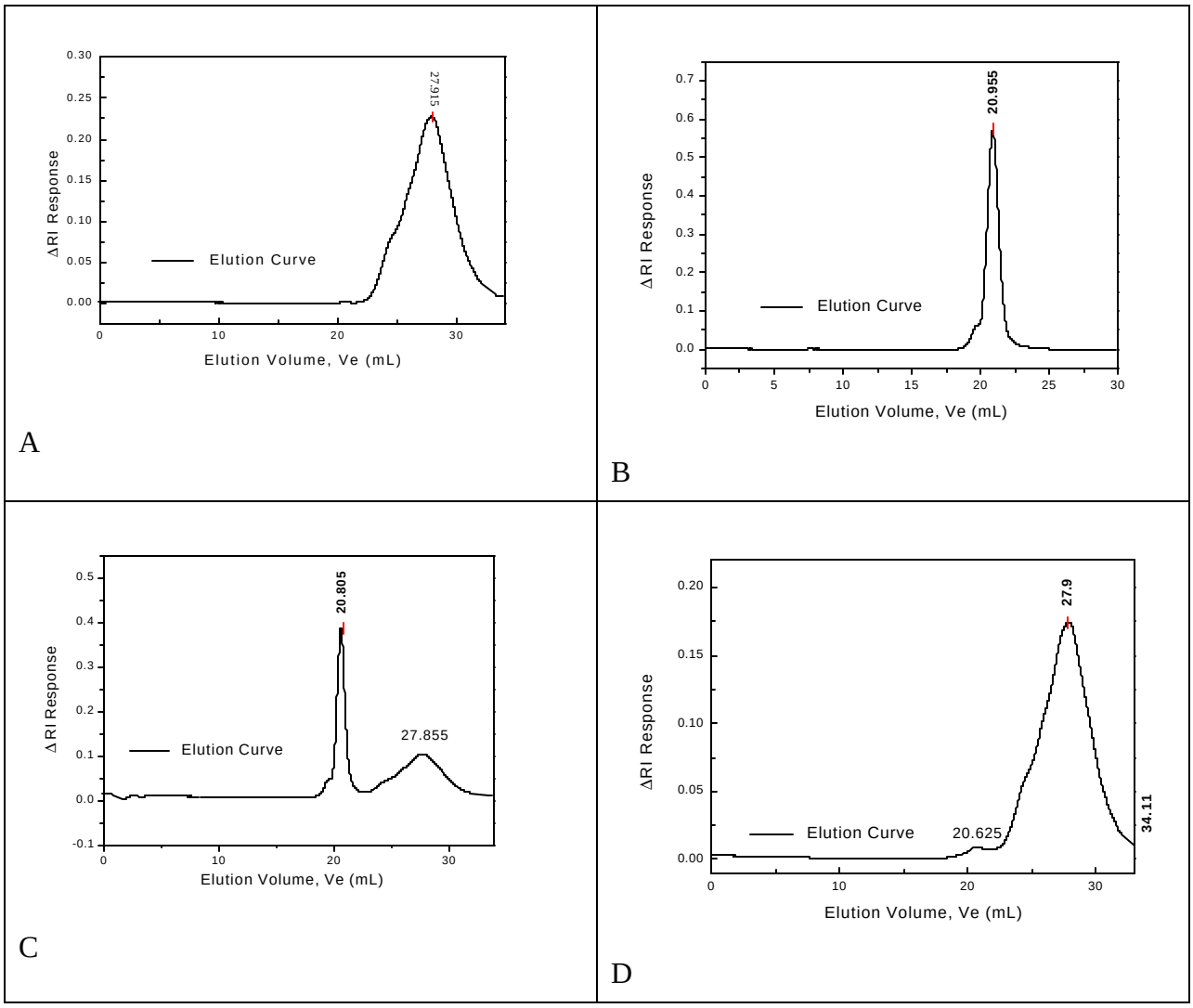

Figure 26
GPC elution peaks of the base asphalt cement for PMAC (A), SBS polymer (B), 1:1 blend of base asphalt and SBS (C), and PMAC samples

clearly separated with a peak centering at 20.62 (Figure 26D). The lower elution volume corresponds to a slight increase in the polymer molecular weight, which might have occurred during the plant preparation of the polymer modified asphalt.

A control sample of AC-30 containing 3 percent SBS was prepared and submitted to TFOT. A new set of columns has been used to develop the GPC chromatogram (Figure 27). Therefore, the elution volumes are slightly different from those reported above for asphalt and SBS samples. The parent asphalt cement (AC-30) eluted in a relatively broad band centering at an elution volume of 21 mL. Each peak in the GPC chromatogram is identified

for both the elution volume and the corresponding molecular weights. In this particular sample, the polymer peak is obvious at an elution volume of 14.2 mL, which corresponds to a peak molecular weight of 120,000 Daltons.

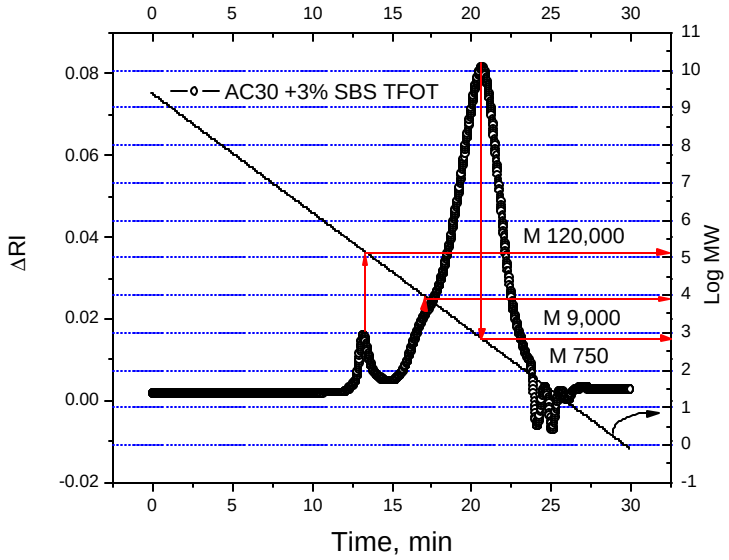

Figure 27
GPC chromatogram of a blend of 3 percent SBS with AC-30 after TFOT

For the analysis of the field aged US61 binder (surface sampled asphalt, top ½ in., labeled as US-61S), the new set of columns was used. In all cases, the parent asphalt cement (AC-30) eluted in a relatively broad band centering at an elution volume between 21.75 mL for the US-61S sample and 21.95 mL for the PMAC, or at a molecular weight of the order of 10^3 Daltons (Figure 28). As expected, aging slightly increased the mean molecular weight of asphalt components, as seen by the shift of PAV-aged PMAC peak to a slightly lower elution volume (21.90 mL). The large differences in the molecular weights between the asphalt and polymer components again allowed baseline separation of the two species in the GPC chromatogram. The polymer species from PMAC eluted at 15.2 mL (Figure 28), which corresponds to a molecular weight of 110,000 Daltons.

The PAV aging process caused a severe oxidation of the PMAC polymer molecules, broadening the peak from 15.2 mL towards higher elution volumes, or lower molecular weights. At the same time, the chromatogram of the US61 surface sampled asphalt showed none of any high molecular species and only a broad shoulder around 19.5 mL (Figure 29).

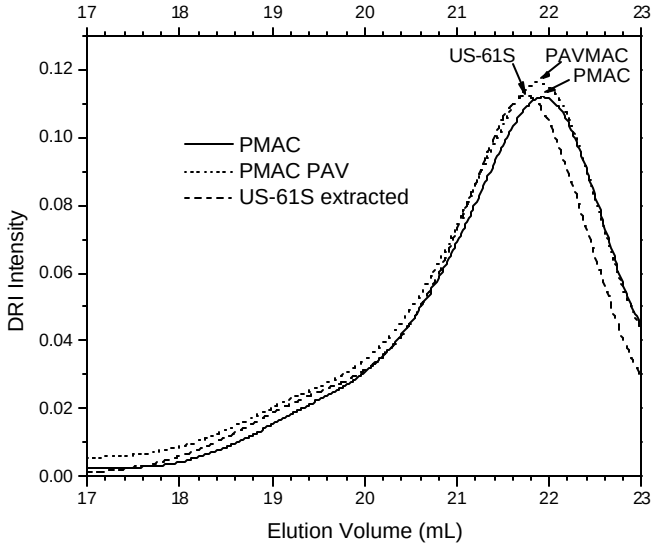

Figure 28

GPC elution peaks of the base asphalt cement for PMAC, PAV aged PMAC, and US-61S binder sampled from the road surface

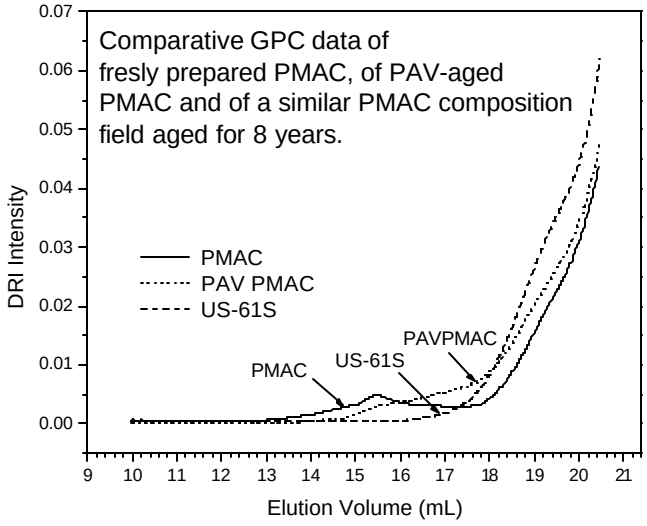

Figure 29

GPC curves at low elution volumes (i.e., high MW) for PMAC, PAV aged PMAC and US-61S binder samples

No residual polymer could be detected in the US-61S bump grind sample even after deconvolution of the peaks (Figure 30). An extensive oxidation of molecular species of the base asphalt as well as polymer degradation presumably occurred in the field-aged samples taken from the road surface.

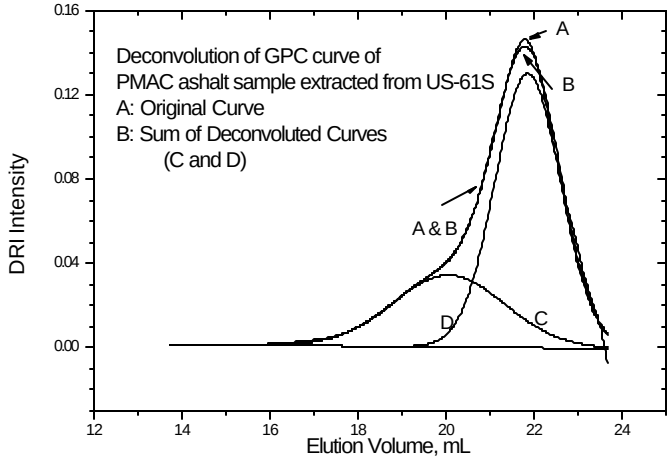

Figure 30
Deconvoluted GPC curves of PMAC, PAV PMAC and US-61S binders

In an effort to ascertain the fate of the polymer additive during oxidation (aging), a PMAC blend containing 3 wt percent SBS was prepared and subjected to TFOT and PAV conditions. At the same time, a new US61 roadway core sample (labeled as US-61C) was taken from beneath the road surface (2 in.). Because a new set of GPC columns were used, analysis included the original PMAC binder and its TFOT and PAV-aged species. Aging dramatically affected the mass of polymeric species (Figure 31). If a peak was still visible after TFOT aging at a high MW corresponding to original rubber, it was diluted towards the higher molecular species of the asphalt. However, a distinct high MW peak in the region of the polymer eluting volumes became visible after deconvoluting the GPC curve of the binder extracted from the US-61C core sample taken from beneath the road surface (Figures 32 and 33).

These preliminary MW data on lab- and road-aged samples show clearly that the current PAV protocol for aging of asphalt cements containing polymeric species, such as SBS, does not accurately reflect the real long term aging process. Further studies to determine the fate of the polymer as the asphalt ages are on-going.

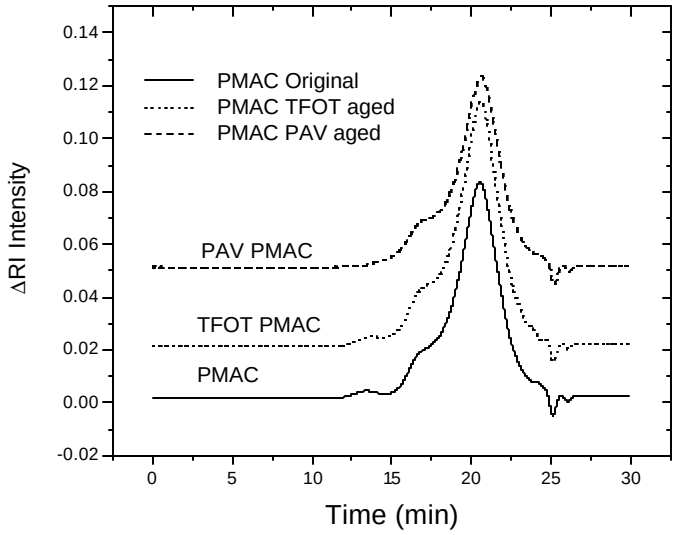

Figure 31
GPC curves for PMAC and its TFOT and PAV-aged species

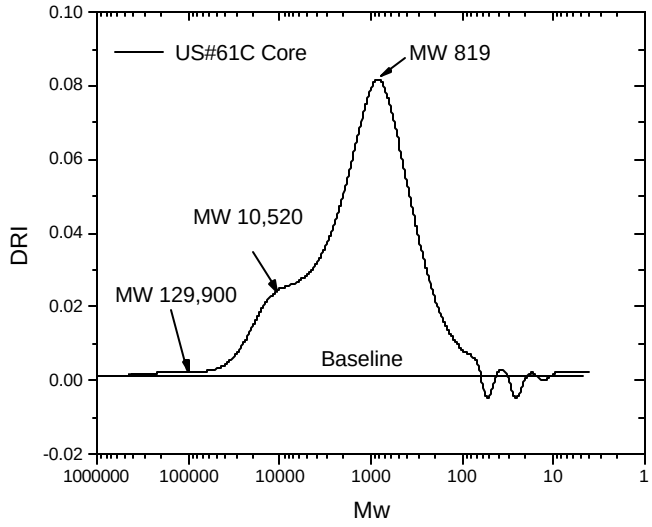

Figure 32
GPC curve of the binder extracted from the US-61C core sample taken from beneath the road surface plotted vs. the MW calibration scale

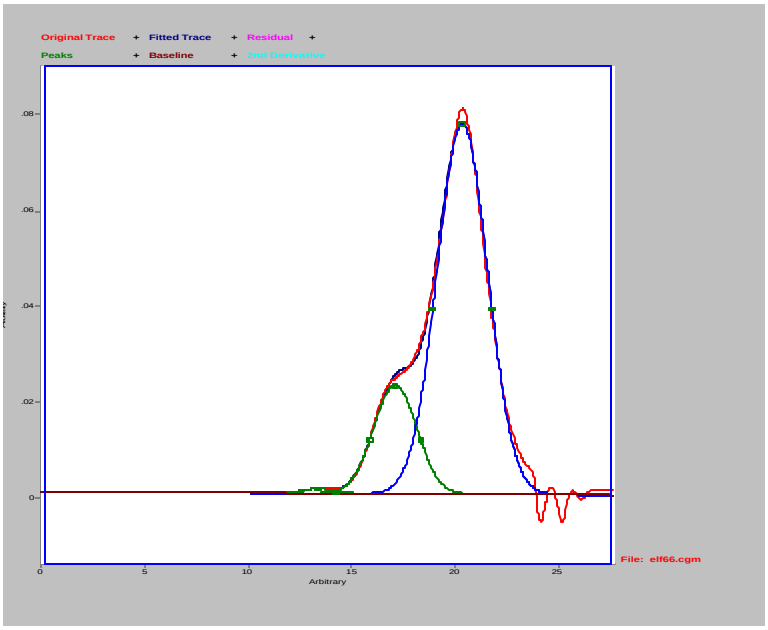

Figure 33

Deconvoluted GPC curve of the binder extracted from the US-61C core sample taken from beneath the road surface showing the peak corresponding to polymeric species

Differential Scanning Calorimetry. Differential scanning calorimetry (DSC) has proved to be a very useful technique for estimating both the crystalline fraction and the glass transition temperature (T_g) of asphalt samples. F. Noel and L. W. Corbett obtained DSC thermograms of asphalts over a broad range of temperatures, enunciated a need to establish a consistent thermal history before comparing different asphalts, and quantified the crystalline components [23]. Blanchard et al. described techniques for measuring glass transition temperatures of asphalt fractions [24]. Claudy et al. devoted great efforts to studying the crystallized fraction in asphalt [25], and Daly et al. showed that the extent of crystallinity of a given asphalt binder can be enhanced by the addition of linear hydrocarbons of similar molecular weight [26].

Using DSC, melting of AC-30 and PMAC crystalline paraffinic species was investigated in the temperature range of 15 to 100°C. The main melting process for an AC-30 sample was observed between 40 to 73°C, with a couple of peaks at 54 and 67°C, respectively (Figure 34). The corresponding heat (enthalpy) of fusion totaled 0.33 mJ/mg, which corresponds to a very low amount of crystalline paraffins in the asphalt composition (melting of paraffinic species 100 percent crystalline, such as linear polyethylene, requires an enthalpy of 200 mJ/mg).

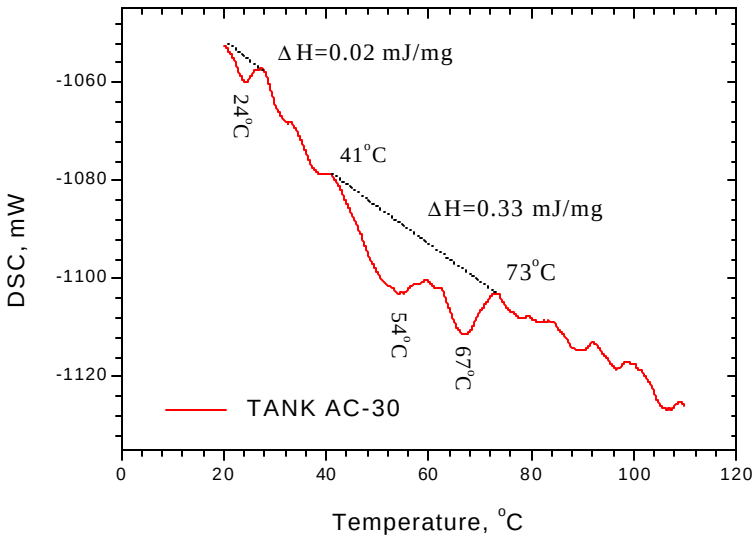

Figure 34
DSC thermogram of AC-30 material

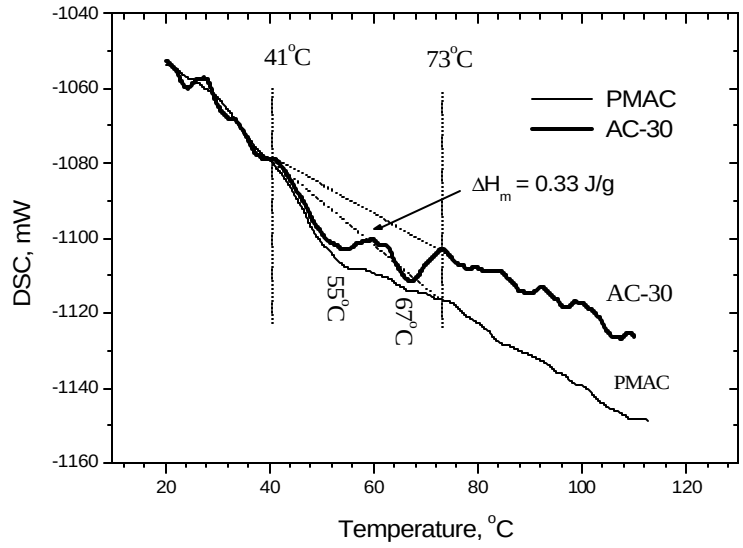

Figure 35
Comparative DSC data of AC-30 and PMAC materials (Traces were normalized to 10 mg for quantitative representation)

The residual crystallinity of AC-30 is still detected in PMAC material after compounding AC-30 asphalt with SBS rubber (Figure 35). Comparatively, the heat of fusion is less (smaller integration area) than that of pure AC-30, but the transition temperatures are the same, i.e., the same crystalline species are present in both materials.

A DSC thermogram of the SBS rubber exhibited only the glass transition, T_g, due to polystyrene blocks at ca. 100°C since the T_g of the polybutadiene blocks fell below the range of temperatures studied (Figure 36).

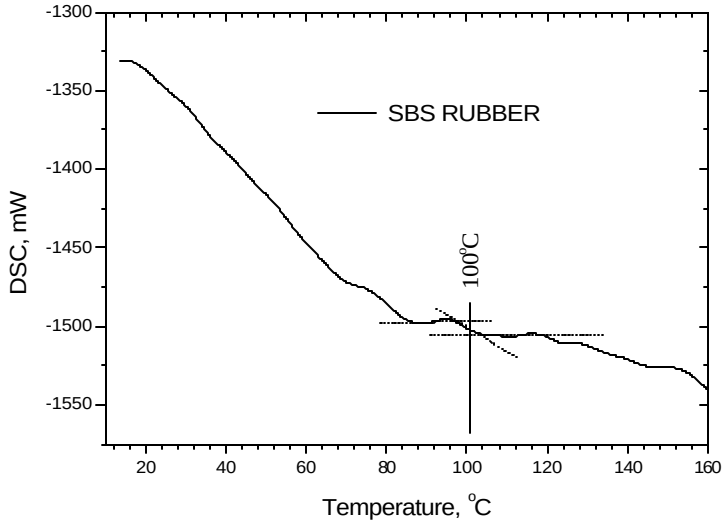

Figure 36
DSC thermogram of SBS styrene-butadiene block copolymer

PAV aging reduced the paraffinic crystallinity of PMAC to one half that of the virgin sample (ΔH_m = 0.16 J/g, Figure 37), rendering a material with good low temperature ductility (see below). On the other hand, the field-aged US61 binder, hard and brittle as compared to the PAV PMAC sample (*vide infra*), was characterized in the same temperature domain by a rather high paraffinic content (ΔH_m = 0.58 J/g, Figure 38). Moreover, the blends containing 20 to 60 percent US-61S binder and PMAC, all hard and brittle at low temperatures as seen by force ductility measurements, had a high paraffinic content, much higher than that given by the simple computation based on their composition. For example, the blend with 60 percent PMAC and 40 percent US-61S material should have a total content of paraffin that melts above 30°C with an enthalpy no higher than 0.43 J/g. However, the melting enthalpy as given by DSC was much higher (ΔH_m = 0.62 J/g, Figure 39), indicating that, in fact, the US-61S components seeded the crystallization of PMAC paraffinic species. Therefore,

despite a high PMAC content, the blends with the field-aged US-61S binder will display an unexpected brittleness at low temperatures.

This brittleness is also related to mobility of asphalt species as reflected by the glass transition, T_g, i.e., the higher the T_g, the more brittle the binder at low temperatures. As expected from mechanical measurements, the glass transition of US-61S binder (T_g= 4.5C, Figure 38) is higher than that of PAV-aged PMAC (T_g= -11C, Figure 37), and correspondingly, the T_g of the blends of US-61S and PMAC are in the range of these two temperatures, viz., the higher the US-61S content, the higher the glass transition.

Measurement of the glass transition of US-61C, even in quenched asphalt samples by DSC is testing the limits of the Universal V2.6D TA instrument. It was not possible to detect the T_g's consistently. An attempt to determine the T_g of an asphalt cement by removing a sample from the asphalt core failed because the concentration of paraffins was too low to detect any thermal transitions. Force ductility or direct tension measurements are better indicators of the T_g of the asphalt matrix. Below the T_g, samples subjected to force ductility underwent brittle fracture. Above the T_g, a ductile fracture was observed (*vide infra*).

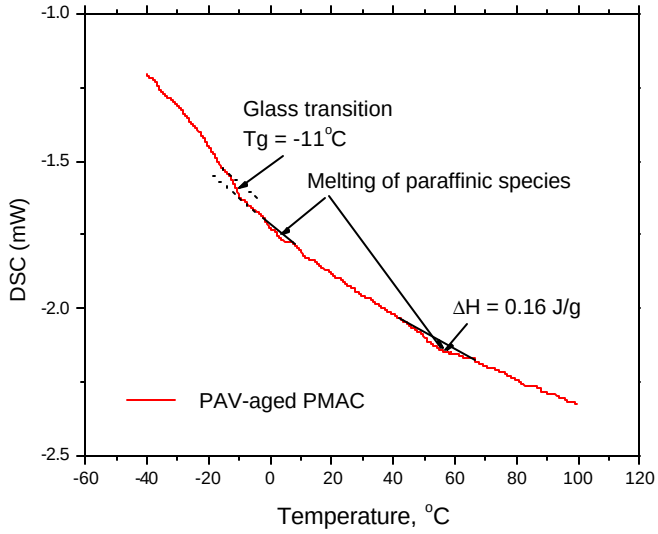

Figure 37
Glass transition and paraffinic crystallinity of PAV aged PMAC

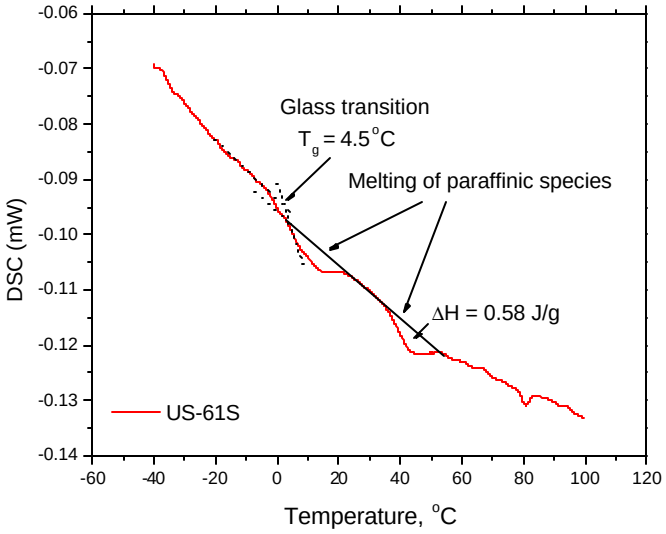

Figure 38
Glass transition and paraffinic crystallinity of US-61S binder

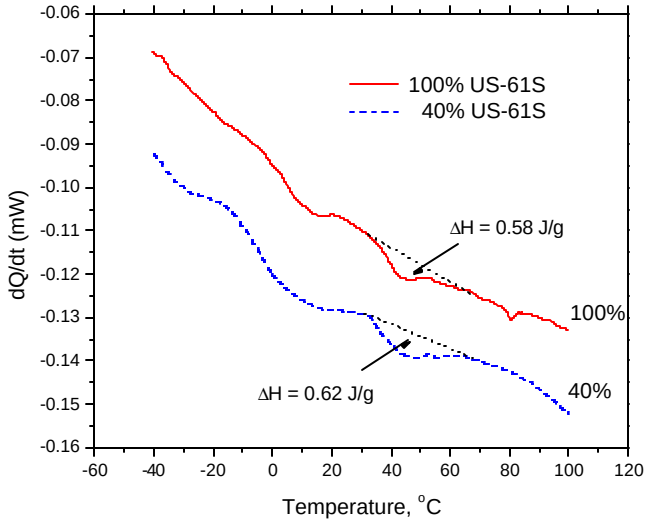

Figure 39
Paraffinic crystallinity of US-61S binder and of the blend containing 40 percent US-61S binder and 60 percent PMAC

The thermal transitions of the asphalt binders are summarized in Table 12. Note the impact of blending on the extent of crystallinity. The presence of polymer in the virgin PMAC lowered the extent of crystallinity. Conversely, the addition of age hardened asphalt components raised the extent of crystallinity in the resultant blend to five times that of virgin PMAC. The increases in crystallinity will increase the tendency of these blends to undergo low temperature cracking and will reduce their fatigue resistance.

Table 12
Thermal transitions of asphalt binders

SAMPLE	Tg °C	Tm1 °C	Tm2 °C	ΔH_{fusion}* mJ/mg
AC-30	**	54	67	0.33
PMAC	**	55	67	0.16
PAV-PMAC	-11.0	56.3	68	0.16
US-61C Binder	4.5	34	81	0.58
20% US61	-0.5	31	60	0.77
40% US61	-3.1	34	60	0.62
60% US61	3.8	30	60	0.56

*Total area of crystalline transitions
**Below -20

Force Ductility. All of the binders containing field-aged asphalts (20, 40, and 60 percent US-61C in PMAC) were too brittle and failed this test at the required temperature, viz., 4°C. They all exhibited a very low ductility (less than 30 percent) and a high load at failure (varying from 180 to 260 lb with the increasing amount of field-aged material in the blend). The lowest temperature at which US-61C passed the test was 15°C (Figure 40). Thus, force ductility data confirmed the positive glass transition temperature of field-aged binders observed by DSC measurements (Figure 38).

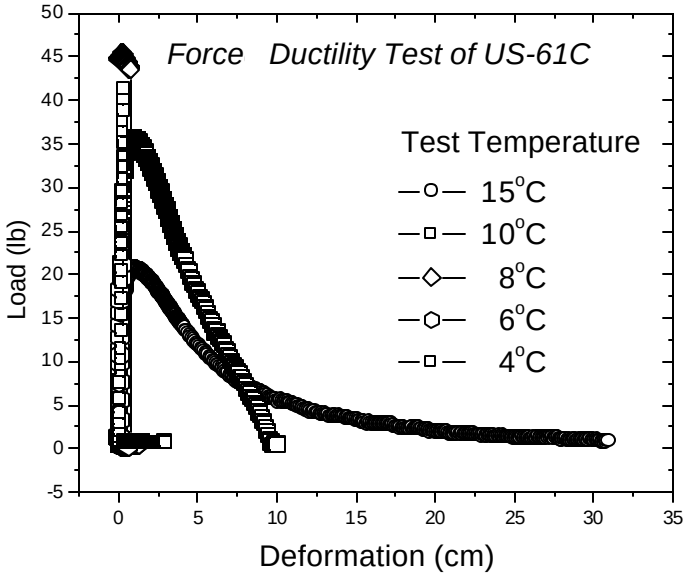

Figure 40
Force ductility data at different temperatures for US-61C binder

Mixture Characterization

Indirect Tensile Strength and Strain Test

The results of the indirect tensile strength and strain (ITSS) test are presented in Figure 41 for the mixtures tested. In general, lab-aged mixtures showed similar ITSS test results as those from field-aged mixtures prepared from US-61S. The indirect tensile strength values increased with the increase of percentage of RPMAC contents for both lab-aged and field RPMAC mixtures.

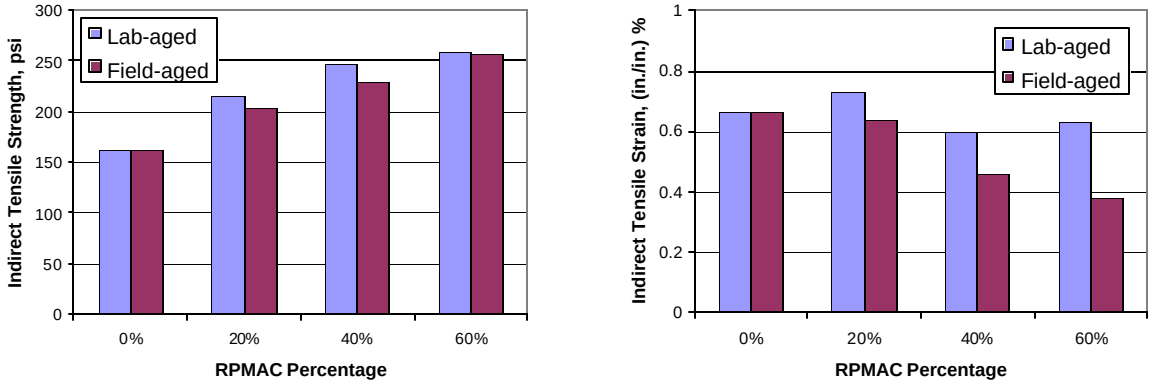

Figure 41
Indirect tensile strength and strain results

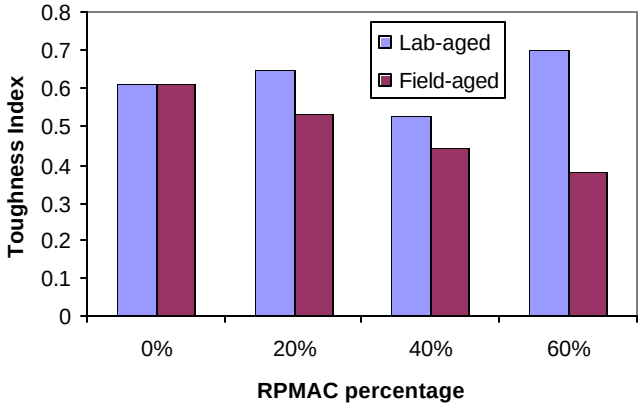

Figure 42
Toughness index

The tensile strains for both mixtures showed a decreasing tendency when more RPMAC was added in the mixture design. Figure 42 presents the computed toughness index (TI) for the mixtures tested. In general, the TI for the mixtures considered decreased with an increase in the percent RPMAC, except for the lab-aged mixture containing 60 percent RPMAC.

Axial Creep Test

Figures 43 and 44 present the results from axial creep tests in this study conducted at 40°C. As shown in Figure 43, field-aged mixtures prepared from US-61S had creep stiffness values higher than or similar to those from lab-aged mixtures, and had creep slope values lower than or similar to those from lab-aged mixtures. Based on the assumption of the axial creep test protocol and the concepts of creep stiffness and creep slope, this finding illustrates that field-aged mixtures had a lower rutting susceptibility than the lab-aged mixtures. The permanent deformation shown in Figure 44 presented the lowest permanent deformation values for all field-aged mixtures, confirming that field-aged mixtures with different RPMAC percentages were stiffer than those from lab-aged and virgin mixtures.

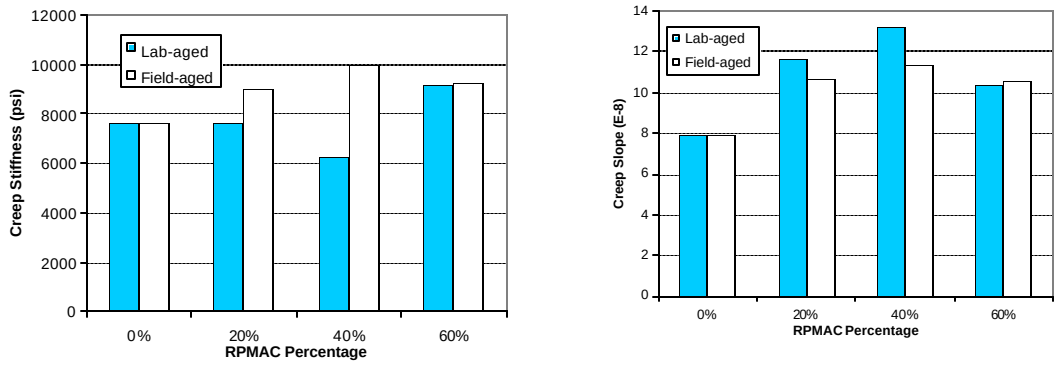

Figure 43
Creep stiffness and slope results from axial creep tests

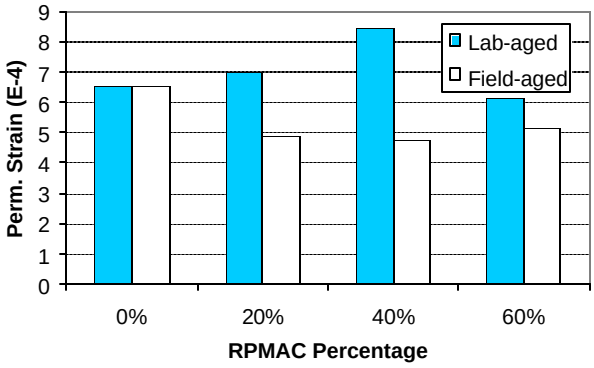

Figure 44
Permanent deformation in axial creep tests

Indirect Tensile Resilient Modulus Test

Figure 45 presents the results of the mean indirect resilient modulus at three temperatures 5°C, 25°C, and 40°C, for the mixture tested. The stiffness of all mixtures, as expected, decreased with an increase in testing temperatures. Also, mixtures containing RPMAC prepared from US-61S consistently showed higher stiffness values than mixtures with no RPMAC.

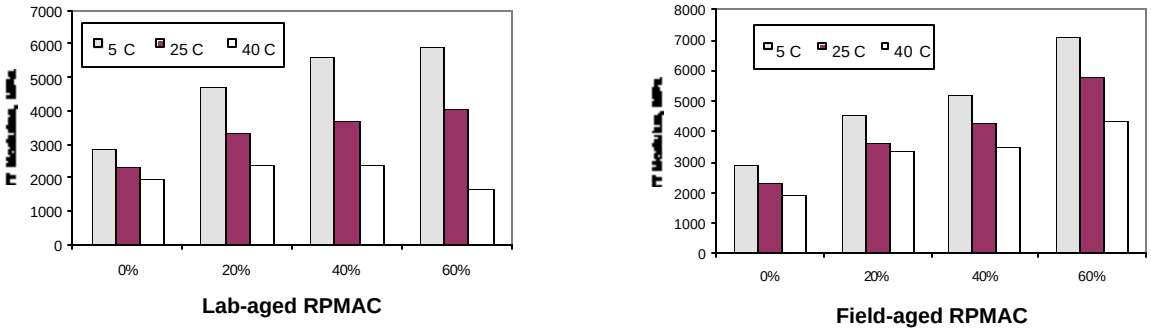

Figure 45
Indirect resilient modulus test

Indirect Tensile Creep Test

Figure 46 shows the mean creep slope of the indirect tensile creep (ITC) test conducted at 40°C. The creep slope for both mixes was considered to be excellent. In general, field-aged mixtures prepared from US-61S showed lower mean creep slopes than lab-aged mixtures and the creep slopes decreased as the percentage of RPMAC used in the mixtures was increased. It is noted that there was no obvious difference in ITC intercept values (initial stiffness) among mixtures without RPMAC contents.

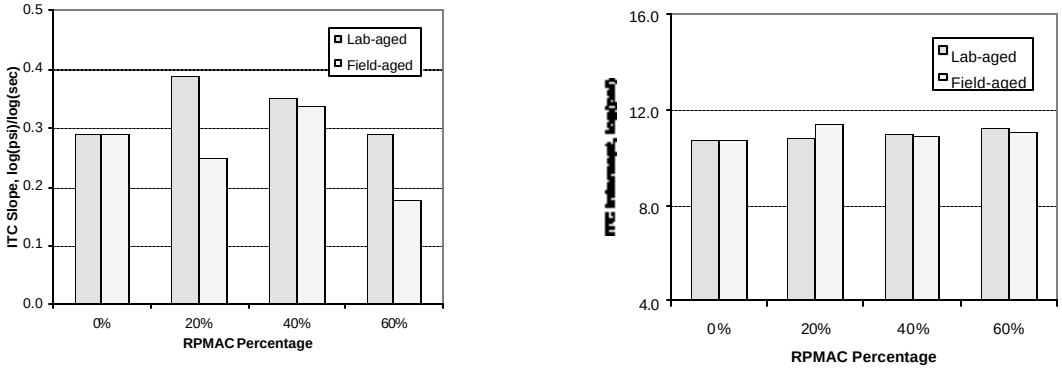

Figure 46
Indirect tensile creep test results

Asphalt Pavement Analyzer (APA) Rut Tester

Figure 47 presents the mean rut depths after 8,000 loading cycles from the APA test conducted at 60°C. Similar to the creep test results, mixtures containing higher RPMAC percentages prepared from US-61S had a higher rut resistance than those mixes with lower RPMAC percentages. This improvement can be attributed to the increased binder stiffness, Table 10. However, the virgin PMAC mixtures showed better rutting resistance than mixtures with 20 and 40 percent RPMAC.

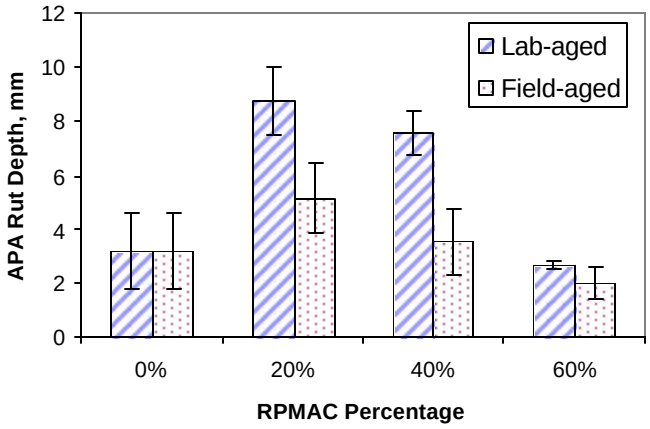

Figure 47
APA rutting test results

Frequency Sweep Test at Constant Height

Figure 48 presents the mean shear complex modulus, G*, at 1 Hz and 10 Hz from the FSCH test conducted at 60°C. In most cases, the shear stiffness obtained from FSCH tests, under both 1 HZ and 10 HZ frequencies, increased as the percentage of RPMAC increased. In general, the shear stiffness values of the field-aged mixtures shared the same increasing trend as those from lab-aged mixtures with some exceptions like the 40 percent field-aged mixture. Field-aged mixtures demonstrated higher complex shear stiffness than lab-aged mixtures.

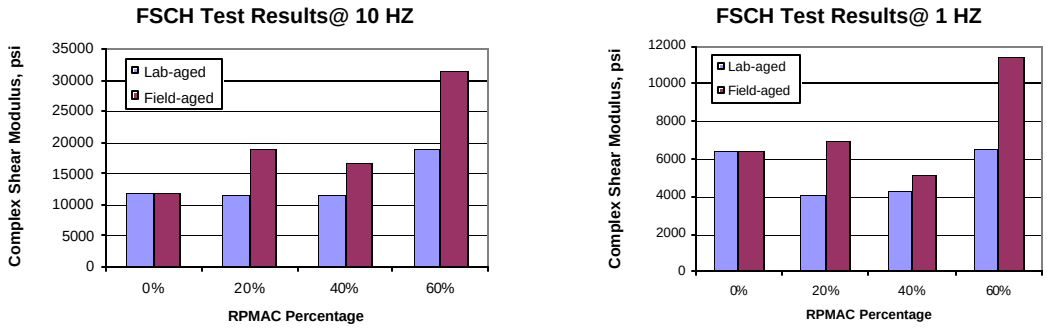

Figure 48
FSCH test results

Repeated Shear Test at Constant Height

A pavement rutting performance prediction model was developed during the SHRP-A003A project. Permanent shear strain obtained from the repeated shear test at constant height can be input into this performance prediction model to predict rut depth as a function of equivalent single axle loads (ESALs). Figure 49 presents the mean permanent shear strains at 5,000 load repetitions from the RSCH test conducted at 60°C. It showed that as the RPMAC percentages increased, the permanent shear strains of both lab-aged and field-aged mixtures decreased, representing a higher rut resistance for high percentage RPMAC mixtures. This finding is consistent with the previously described APA and FSCH test results. Again, the zero percent RPMAC mixture or mixtures with virgin PMAC binder showed slightly lower permanent shear strain values than those lab-aged mixtures with 20 and 40 percent RPMACs.

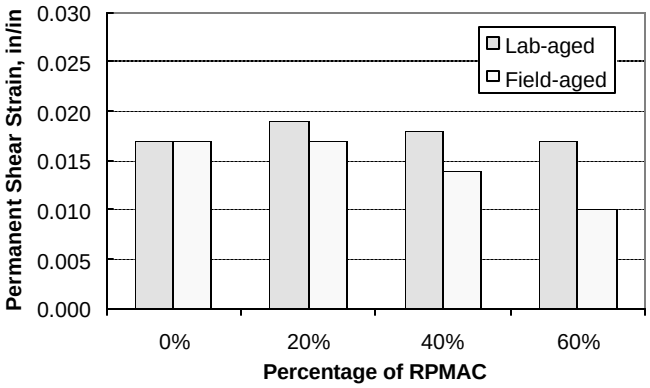

Figure 49
Permanent shear strain from RSCH test

Simple Shear Test at Constant Height

Figures 50 and 51 present the test results from the SSCH test conducted at 60°C. It showed that as the percentages of RPMAC increased, both the permanent shear strains and the maximum shear strains for both mixtures decreased, representing better rut resistance for high percentage RPMAC mixtures. Field-aged mixtures prepared from US-61S consistently showed lower permanent shear and maximum shear strain values, which seemed to illustrate that the lab-aging procedure failed to represent the field aging conditions. More research is needed in this area.

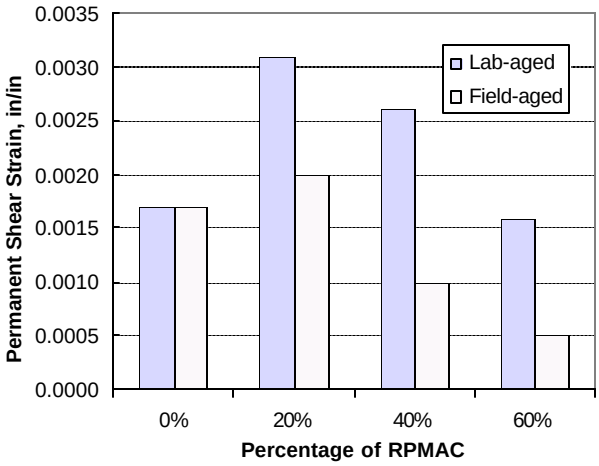

Figure 50
Permanent shear strain from SSCH tests

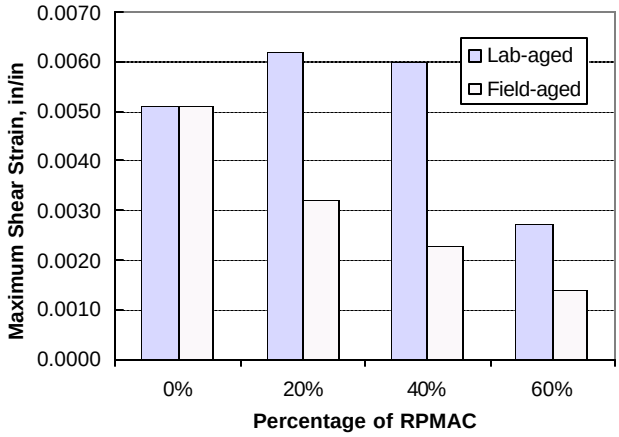

Figure 51
Maximum shear strain from SSCH tests

Semi-Circular Fracture Test

The average values of fracture energy (U) are plotted versus different notch depths to compute the slope of a regression line, which is the value of (dU/da) in Equation (5). Figure 52 presents the (dU/da) results for the four asphalt mixtures (field-aged) considered in this study. The critical value of facture resistance, J_c, is then computed by dividing the dU/da value by the specimen width, b.

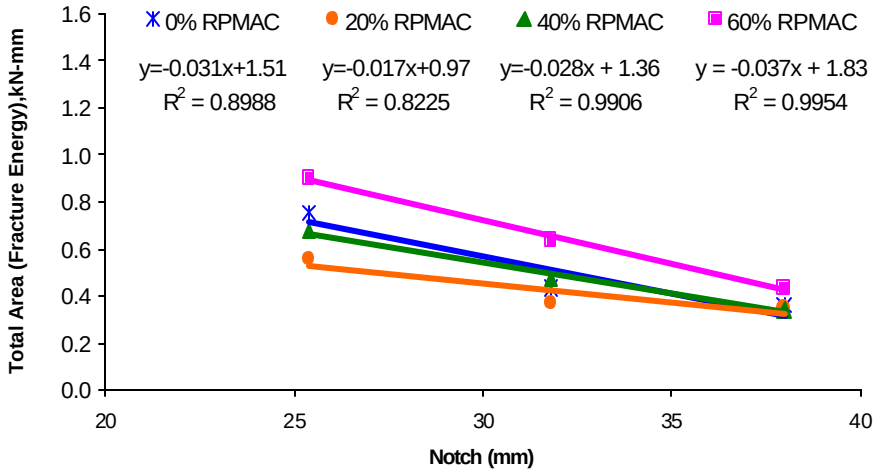

Figure 52

Variation of Fracture Energy with notch depth

Table 13 presents the computed critical fracture resistance of J_c for each of the four RPMAC Superpave mixtures considered. Also shown in Table 13 are some critical fracture resistance data from other studies [19, 28].

Table 13

Comparison of the Critical Fracture Resistance for various asphalt mixtures

	0%	20%	40%	60%	Control PG 70-28	CRA PG 70-22	AC-5 +5% SEBS	AC-5 +2% Elvaloy
J_c (kJ/m^2)	0.55	0.30	0.48	0.65	0.54	0.65	0.42	0.48
	Current RPMAC study				(Mull et al., 2002)		(Bhurke et al., 1997)	

The J_c values from current RPMAC study are comparable with that from other studies, Table 13. Further confidence is gained from the fact that bending beam specimens were used in the study by Bhurke et al. (1997) [28]. The mixture without RPMAC (0 percent) has almost the same J_c as that reported by Mull et al. [19] for PG 70-28. When a 20 percent recycled asphalt was used the value of J_c dropped considerably, from about 0.55 kJ/m^2 for the 0 percent RPMAC to about 0.30 kJ/m^2 for the 20 percent RPMAC. As the percentage of the recycled

polymer asphalt cement increased past 20 percent RPMAC, the J_c increased. It reached 0.48 kJ/m^2 at 40 percent RPMAC and 0.65 kJ/m^2 at 60 percent RPMAC.

It is well documented that as asphalt binders age, some of the molecules become oxidized, which results in strongly interacting functional groups that contain oxygen [29]. Exposure of the pavement to ultraviolet light [30] as well as oxygen diffusion through air voids [31] appear to be the main causes of asphalt oxidation [32]. In this study, the increased stiffness of RPMAC binders (Table 8) and the decreased indirect tensile strain of RPMAC mixtures (Figure 41) exactly reflected the age-hardening of RPMAC due to the oxidization. It is generally believed that the age-hardening of asphalt binders will increase the tendency of an asphalt mixture to undergo low temperature cracking and also reduce its fatigue resistance. However, the fracture resistance test results in this study tend to disagree with this statement. As shown in Table 13, the value of J_c first drops from 0 percent RPAMC to 20 percent RPMAC; then it continuously increases as the RPMAC binder content increases. Since the value of J_c represents the fracture resistance of a material, larger values mean better fracture resistance. Therefore, the results in Tables 13 indicate that the 60 percent RPMAC mixtures have a better fracture resistance than 0 percent, 20 percent and 40 percent RPMAC mixtures.

This observation initially appears abnormal. However, a similar observation of the effect of an SBS modifier on the fracture and fatigue behavior was also made by Aglan et al. (1993) [33] using an AC-5 base asphalt. They found that as the dosage of modifier was increased, a stiffer and stronger asphalt mixture was obtained. This was accompanied by a slight decrease in the deflection at maximum load, yet an overall increase in the fracture and fatigue resistance was reported. This trend is the same as seen in the current study. Moreover, the sudden drop of the value of J_c from 0 percent RPMAC mixture to that of 20 percent could be due to the fact that the RPMAC at low concentrations is incompatible with the controlled elastomeric modified binder (PMAC in this study). It appears that the 20 percent RPMAC has created some sort of discontinuity, which weakened the adhesive and cohesive properties of the binder and promoted the crack propagation in the mixtures. As more RPMAC was added, its stiffening effect overcame that of the new control modified binder. This was accompanied by an increase in the maximum sustained load and slight decrease in the deflection at maximum load. The increased load and small decrease in deflection has resulted in an increase in the values of strain energy to failure, U. As a matter of fact, field observations supported J-integral test results that aged RPMAC mixtures produced better or same fracture resistance than the original PMAC mixtures [27].

It should be noted that the value of J_c represents the fracture resistance of a material under monotonic loading (load excursion). It does not directly reflect the durability or fatigue damage tolerance of a material. Nevertheless, it can be a valuable correlative tool in fatigue crack growth studies. Thus, it is equally important to study the fatigue crack propagation behavior of the asphalt mixtures under consideration using the proposed semicircular specimen and the J-integral concept.

Beam Fatigue Test

The beam fatigue test results for lab-aged and field-aged (US-61S binder) Superpave mixtures are shown in Figures 53 and 54, respectively. As expected in the indirect tensile strength and strain tests, the general trend of fatigue resistance for mixtures with various RPMAC binder contents should be 0, 20, 40 and 60 percent. As seen in Figure 54, the zero percent RPMAC mixture showed better fatigue cracking resistance in terms of longer fatigue life than any other mixtures shown in the figure. A reduced cracking resistance observed for mixtures containing 20 and 60 percent US61 binders would be expected. It is noted that the fatigue curve for mixtures containing 40 percent of US61 binder was found to deviate from the trend observed with the 20 and 60 percent mixtures. Excessive aging during the sample handling and heating in this mixture may be the reason for this inconsistency.

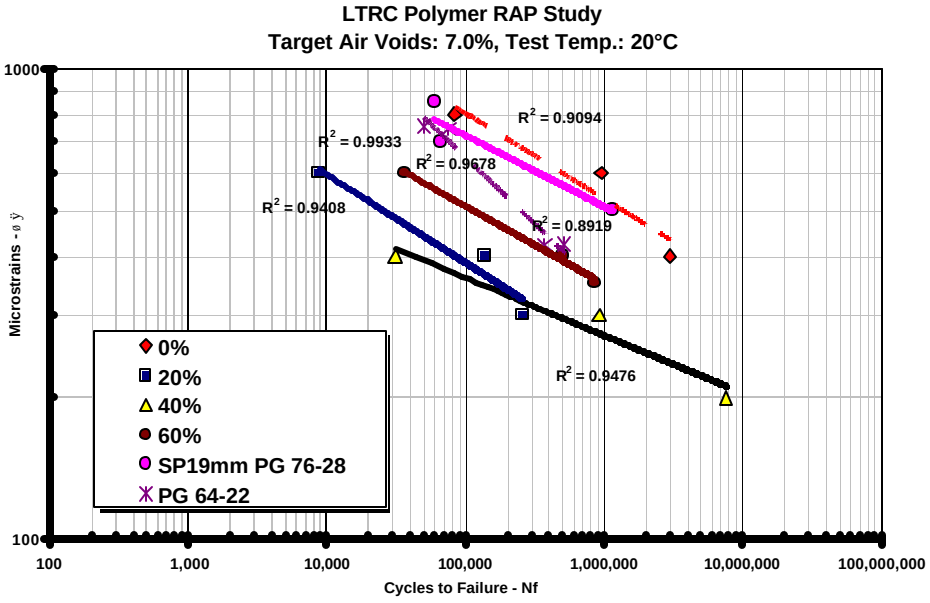

Figure 53
Fatigue test result (lab-aged RPMAC)

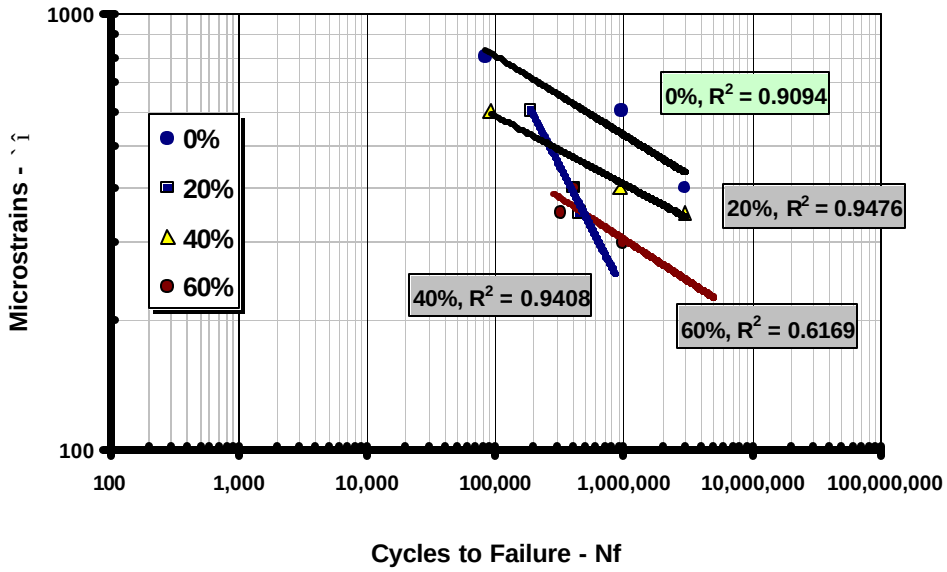

Figure 54
Fatigue test result (field-aged RPMAC)

Effects of Binder Performance Characteristics on Mixture Performance

Permanent Deformation

Figure 55 shows the relationship between the binder rutting factor of G*/sin(δ) at 64°C and the APA rut depths of mixtures containing various percentages of the US-61S binder. The temperature of 64°C was selected because the APA test was conducted at this temperature. The graph shows that the rutting factor of G*/sin(δ) is very sensitive to the APA rut depth and the G*/sin(δ) is inversely proportional to the APA rut depth. This is expected since as the binder high temperature stiffness, G*/sin(δ), increases, the rut resistance of mixtures will also increase and thus produce a lower APA rut depth. Similar relationships can also be found between the G*/sin(δ) and the creep slope of the IT creep test (Figure 56), and between G*/sin(δ) and the permanent shear strain in the RSCH test (Figure 57). Therefore, it is concluded that the binder rutting properties are reflected in the mixture properties and the binder rutting factor of G*/sin(δ) is very sensitive to the permanent deformation properties of asphalt mixtures containing recycled PMAC binders.

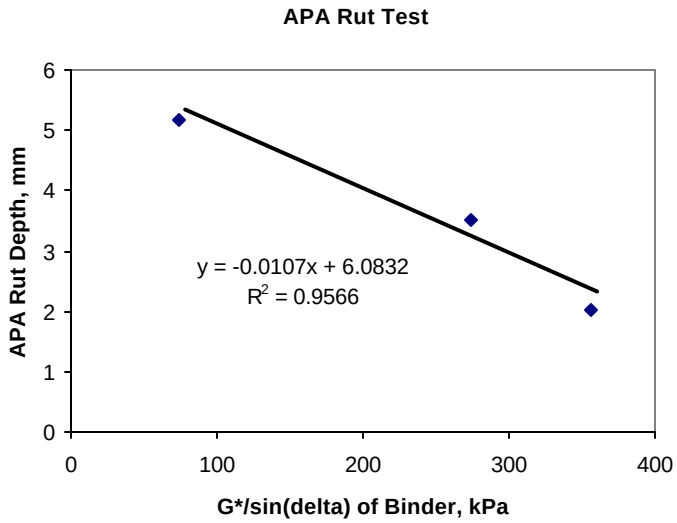

Figure 55
G/sin(d) of binder vs. APA rut depth

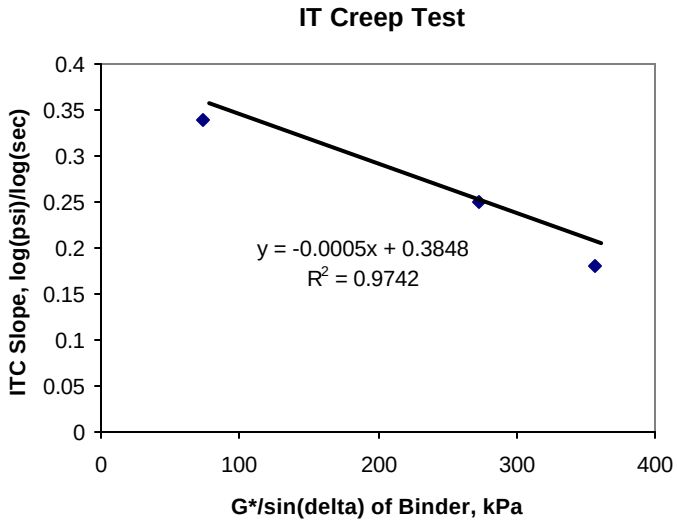

Figure 56
G/sin(d) of binder vs. creep slope in ITC test

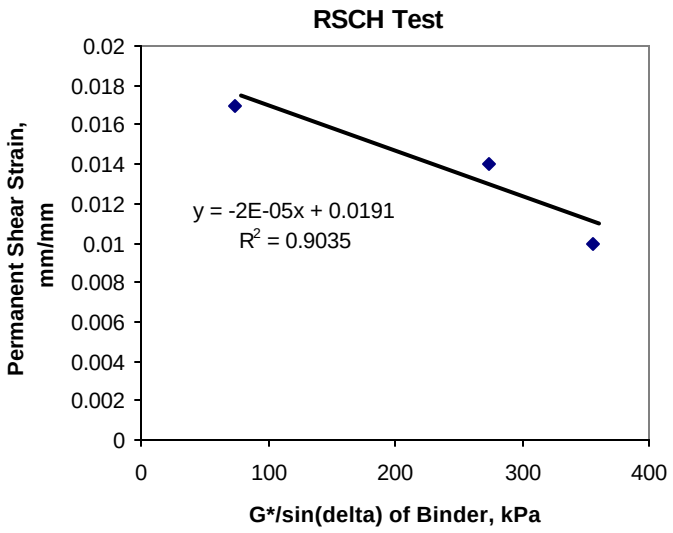

Figure 57

G/sin(d) of binder vs. permanent shear strain in RSCH test

Fatigue Cracking

Figure 58 presents the binder fatigue parameter, G*sin(δ) at the temperature of 25°C versus the toughness index (TI) of mixtures containing various percentages of the US-61S binder. Beam fatigue test results were not considered because of the inconsistent results from mixtures containing 40 percent US61 binder, which was mainly due to the improper reheating during the sample handling, as stated before. The temperature of 25°C was selected because the indirect tensile strength and strain test was conducted at this temperature and TI values were computed from the test results. As shown in Figure 58, a strong correlation was observed between the G*sin(δ) and the TI values. As the G*sin(δ) at the intermediate temperature (e.g. 25°C) increases, the binder becomes brittle and has a high potential for fatigue cracking; a mixture containing such a binder will also have a high potential for fatigue cracking, which will result in a low TI value, as expected. Therefore, it is concluded that the binder fatigue properties are reflected in the mixture fatigue properties, and the binder fatigue parameter of G*sin(δ) is sensitive to the fatigue properties of asphalt mixtures containing recycled PMAC binders.

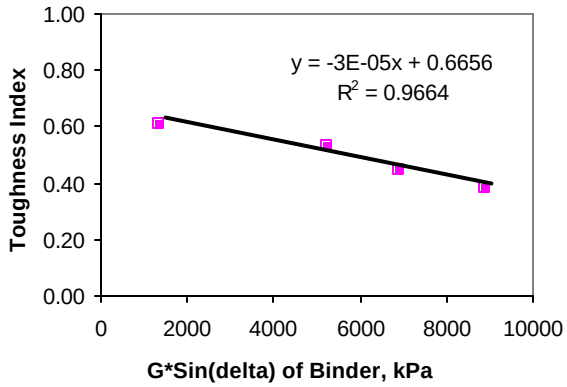

Figure 58
G*sin(d) of binder at 25°C vs. toughness index

Development of Nomograph for blending RPMAC

To construct a blending chart, the desired final binder grade and the physical properties (and critical temperatures) of the (RPMAC) recovered binder were needed, along with one of the following pieces of information (NCHRP Report 452):

- The physical properties (and critical temperatures) of the virgin binder, or
- The percentage of RAP in the mixture.

Once the RAP binder was extracted and recovered, its properties needed to be determined. The RAP binder had to be tested in the dynamic shear rheometer (DSR) at a high temperature as if it were the original, un-aged binder. Then the remaining RAP binder was aged in the rolling thin film oven (RTFO) and was tested in the DSR and bending beam rheometer (BBR).

RAP Testing Protocol

The following six steps were followed to determine the physical properties and critical temperatures of the RAP binder.

1. Original DSR testing was performed on the recovered RAP binder to determine the critical high temperature, $T_c(High)$, based on original DSR values where $G^*/\sin\delta$ = 1.00 kPa. The critical high temperature was calculated as follows:
   1.1 The slope of the stiffness-temperature curve was determined as $\Delta Log(G^*/\sin\delta)/\Delta T$.

1.2 $T_c(High)$ was determined to the nearest 0.1°C using the following equation:

$$T_c(High) = \{[\text{Log}(1.00) - \text{Log}(G1)]/a\} + T_1 \quad (6)$$

Where:

G_1 = the $G^*/\sin\delta$ value at a specific temperature, T_1, and

a = the slope of the stiffness–temperature curve described in (1.1).

Although any temperature (T_1) and the corresponding stiffness (G_1) could have been selected, the G*/sin d value closest to the criterion (1.00 kPa) was used to minimize extrapolation errors.

2. RTFO aging was performed on the remaining RAP binder.

3. DSR testing was performed on the RTFO-aged recovered RAP binder to determine the critical high temperature (based on RTFO DSR). The critical high temperature (based on RTFO DSR) was calculated as follows:

3.1 The slope of the stiffness-temperature curve was determined as $\Delta\text{Log}(G^*/\sin\delta)/\Delta T$

3.2 $T_c(High)$, based on RTFO DSR, was determined to the nearest 0.1°C using the following equation:

$$T_c(High) = \{[\text{Log}(2.20) - \text{Log}(G1)]/a\} + T_1 \quad (7)$$

Where:

G_1 = the $G^*/\sin\delta$ value at a specific temperature, T_1, and

a = the slope of the stiffness–temperature curve described in step 3.1.

Although any temperature (T_1) and the corresponding stiffness (G_1) could have been selected, the G*/sin d value closest to the criterion (2.20 kPa) was used to minimize extrapolation errors.

4. The critical high temperature of the recovered RAP binder was determined as the lower of the original DSR and RTFO DSR critical temperatures. The high-temperature performance grade of the recovered RAP binder was determined based on this single critical high temperature.

5. The intermediate temperature DSR testing on the RTFO-aged recovered RAP binder was performed to determine the critical intermediate temperature, $T_c(Int)$, based on pressure aging vessel (PAV) DSR.

5.1 The slope of the stiffness-temperature curve was determined as $\Delta\text{Log}(G^*\sin\delta)/\Delta T$

5.2 $T_c(Int)$, based on RTFO DSR, was determined to the nearest 0.1°C using the following equation:

$$T_c(Int) = \{[\text{Log}(5000) - \text{Log}(G1)]/a\} + T_1 \quad (8)$$

Where:

G_1 = the $G^*\sin\delta$ value at a specific temperature, T_1, and
a = the slope of the stiffness–temperature curve described in step 5.1.

Although any temperature (T_1) and the corresponding stiffness (G_1) could have been selected, the G*sin d value closest to the criterion (5000 kPa) was used to minimize extrapolation errors.

6. BBR testing was performed on the RTFO-aged recovered RAP binder to determine the critical low temperature, $T_c(S)$ or $T_c(m)$, based on BBR stiffness or *m*-value.

6.1 The slope of the stiffness-temperature curve was determined as $\Delta\text{Log}(S)/\Delta T$.

6.2 $T_c(S)$ was determined to the nearest 0.1°C using the following equation:

$$T_c(S) = \{[\text{Log}(1.00) - \text{Log}(S_1)]/a\} + T_1 \quad (9)$$

Where:

S_1 = the *S*-value at a specific temperature, T_1, and
a = the slope of the stiffness–temperature curve described in step 6.1.

Although any temperature (T_1) and the corresponding stiffness (S_1) could have been selected, the S-value closest to the criterion (300 MPa) has been used to minimize extrapolation errors.

6.3 The slope of the *m*-value-temperature curve was determined as $\Delta m\text{-value}/\Delta T$.

6.4 $T_c(m)$ was determined to the nearest 0.1°C using the following equation:

$$T_c(m) = \{[\text{Log}(0.300) - \text{Log}(m_1)]/a\} + T_1 \quad (10)$$

Where:

m_1 = the *m*-value at a specific temperature, T_1, and
a = the slope of the curve described in step 6.3.

Although any temperature (T_1) and the corresponding m-value (m_1) could have been selected, the m-value closest to the criterion (0.300) has been used to minimize extrapolation errors.

6.6 The higher of the two low critical temperatures $T_c(S)$ and $T_c(m)$ was selected to represent the low critical temperature for the recovered asphalt binder, $T_c(Low)$. The low-temperature performance grade of the recovered RAP binder was determined based on this single critical low temperature.

Blending Protocols

Once the physical properties and critical temperatures of the recovered RAP binder were known, two blending approaches could have been used. In one approach (designated *Method A*), the percentage of RAP to be used in an asphalt mixture was known, and the appropriate virgin asphalt binder grade for blending needed to be determined. In the second approach (designated *Method B*), the maximum percentage of RAP that can be used in an asphalt mixture while still using the same virgin asphalt binder grade needed to be determined. Both approaches assumed that the performance grade of the final blended binder was specified.

In the present study *Method B* was selected for blending the US-61C with a known virgin binder grade (RAP percentage unknown). Using the following equation for the high, intermediate, and low critical temperatures separately, the percentage of RAP needed to satisfy the assumptions can be determined.

$$\%\text{RAP} = (T_{\text{Blend}} - T_{\text{Virgin}})/(T_{\text{RAP}} - T_{\text{Virgin}}) \quad (11)$$

This equation was obtained by rearranging equations 1-5 for critical temperatures.

Application of Nomogram

The materials used for developing the nomogram study were:

- RAP: a polymer modified (SBS) asphalt binder extracted from US61 core samples and characterized as a PG 82-10 binder (US-61C).
- Virgin asphalt cement: an asphalt cement characterized as a PG 58-28 binder.
- The target grading was set as PG 70-22.

The Superpave grading procedure was performed on both binders. The PG 58-28 binder was blended with 3 percent SBS rubber by stirring the asphalt and the polymer for ca. 2 hours at 175^{o}C under nitrogen atmosphere. Following the procedure, all calculations for known binder properties and unknown RAP content were done as described above. According to the calculations, a blend of US-61C and virgin asphalt (PG 58-28) containing 37 to 55 percent RAP should produce the formulation needed to obtain the target grading of PG 70-22.

A Superpave grade determination procedure was performed on a 37.35 percent wt US-61C blend (minimum content of RAP according to nomogram) with PG 58-28 virgin asphalt to check the correlation between mathematical and experimental results. The blend (nomogramix) failed to reach the specifications for PG 70-22 on the TFOT DSR test (Table

14). This result indicates that more than 3 percent rubber must be blended with the virgin asphalt in order to make up for the lost rubber in the US-61C, particularly from the surface asphalt layers (see GPC data).

Table 14
Critical temperatures and performance grading of asphalts for recycling of US-61C asphalt pavement in a new asphalt composition

Critical temperatures °C	**US-61C**	**PG 58-28**	**PG 58-28 3%SBS**	**37.35% US61 RAP Blend**
DSR original binder	87.8	57.6	59.5	72.4
DSR TFOT	86.2	54.7	60.6	67.2
DSR PAV	31	19.3	12.9	20.6
BBR – m	-4.98	-21.02	-20.5	-16.91
BBR – S	-9.99	-20.3	-28.23	-19.67
PG Grading	**82 – 10**	**52 – 28**	**58 – 28**	**64 – 22**
TARGET				**70 – 22**

SUMMARY AND CONCLUSION

A 19 mm Superpave mixture was designed for use in the laboratory evaluation. Fundamental characterization for binders utilizing 0, 20, 40, and 60 percent of reclaimed polymer-modified asphalt cement (RPMAC) were conducted. This included Superpave binder PG rheology evaluation. In addition, mixture characterization was performed using the Superpave test protocols, indirect tensile strength and strain, resilient modulus, creep, semi-circular fracture and loaded wheel tests. In general, the addition of RPMAC in a Superpave mixture design improved the mixture's performance in terms of its rutting resistance and possibly also its fracture resistance (especially at high RPMAC contents), but the RPMAC seemed to decrease the Superpave mixture's fatigue endurance.

Following are the major observations and findings made from this project:

- An efficient extraction technique for removing aged asphalt binder from the aggregate in asphalt concrete mixtures was developed. The impact of the extraction and recovery process on binder properties was ascertained and found to be minimal.
- Procedures were developed to separate the PMAC into its asphalt resin and polymer additive components. These procedures will be useful in ascertaining the quality of PMAC purchased by LADOTD.
- Laboratory evaluation showed that the use of RPMAC in a Superpave mixture design did improve the mixture's rutting resistance. The higher the percentage of RPMAC, the better the rutting resistance of the mixtures.
- Aging properties of the PAV-aged PMAC and US61 binders were characterized with the FTIR spectroscopy test. The oxidization of each asphalt binder was identified by a large set of peaks (which corresponded to carbonyl absorptions of oxidized species) in the infrared spectra data. The results showed that the US61 binder exhibited a higher extent of oxidation than the PAV-aged PMAC. As the percentage of US61 binder mixed with virgin PMAC binder increased, higher oxidation was observed in the infrared spectra data.
- Gel permeation chromatography (GPC) failed to detect residual polymer in the US61 roadway binder extracted from the road surface. Extensive aging of molecular species led to either polymer degradation or extensive crosslinking, which rendered the polymer component insoluble.
- The DSC analysis showed that the PAV aging process reduced the paraffinic crystallinity of PMAC to one half that of the virgin sample. However, the field-

aged US61 binder was found to have the increased paraffinic crystallinity, which caused it to be relatively hard and brittle as compared to PAV PMAC sample.

- The blends containing 20 to 60 percent US-61S binder and the virgin PMAC were found to contain much higher paraffinic contents than the simple computation based on their composition. It is believed that the US61 components seeded the crystallization of PMAC paraffinic species. Therefore, despite a high PMAC content, the blends with the field-aged US61 binder displayed an unexpected brittleness at low temperatures.
- This brittleness of the binder can be related to asphalt species' mobility as reflected by the glass transition. The higher the glass transition temperature, the more brittle the binder was at low temperatures. The glass transition temperature of the US61 binder was higher than that of PAV-aged PMAC; thus, the higher the US61 content in the blends of US61 and PMAC, the higher the glass transition of the binder. The increases in glass transitions and in crystallinity will increase the tendency of these blends to undergo low temperature cracking and will reduce their fatigue resistance.
- Results of the mixture performance tests showed that increasing the percentage of US61 binder in mixtures would increase the rutting resistance but decrease the fatigue resistance of the recycled PMAC mixtures.
- Both Superpave PG binder's rutting factor of $G^*/\sin(\delta)$ and fatigue parameter of $G^*\sin(\delta)$ were found to be fairly sensitive to performance properties of asphalt mixtures containing recycled PMAC binders.
- Laboratory evaluation indicated that the addition of RPMAC did not improve the mixture's fatigue endurance. All mixtures containing RPMAC had lower fatigue lives than the mixtures with virgin binder (zero percent RPMAC). However, a mixture containing 60 percent RPMAC exhibited better fatigue life than those mixtures with 20 and 40 percent RPMAC, suggesting that there is a threshold value for using RPMAC in a Superpave mixture design. Mixtures with RPMAC contents lower than the threshold content will sacrifice their fatigue lives.
- The semi-circular fracture test results indicated that an increased percentage of RPMAC in an asphalt mixture exhibited higher critical fracture resistance value, J_c. It is believed that as more RPMAC was added, its stiffening effect overcame that of the new control modified binder. This was accompanied by an increase in the maximum sustained load and a slight decrease in the deflection at maximum load. The increased load and small decrease in deflection has resulted in an increase in the values of strain energy to the failure, U, and the critical value of fracture resistance, Jc. This study suggests that semi-circular fracture test can be

used as a valuable correlative tool in predicting fracture resistance of asphalt mixtures.

RECOMMENDATIONS

This study demonstrated that the current laboratory aging procedures (TFOT and PAV) failed to predict the aging of PMACs in the field. It is noted that the rate of change of aging, rather than absolute aging, is a better rheological approach in measuring binder contribution to the durability of asphalt mixtures. First, the most relevant time-dependent rheological properties must be ascertained. Then, a method for aging large quantities of PMAC that will allow multiple sampling over time must be employed. Sampling should be conducted until the effect of aging within a typical time period is minimal. When the rate of change of aging reaches a plateau, the aged sample can then be graded, and a nomogram is used to select the appropriate blend of RPMAC and asphalt binder to produce recycled asphalt cement.

Based on the findings of this research the following is recommended for implementation:

A. The extraction procedure that was developed for removing aged asphalt binder from the aggregate;
B. The gel permeation chromatography procedures that were developed for separating the PMAC into its asphalt resin and polymer additive components. These procedures are useful in ascertaining the quality of PMAC purchased by LADOTD; and
C. The design method of the use of RPMAC as described in NCHRP report number 452 "*Recommended Use of Reclaimed Asphalt Pavement in the Superpave Mix Design Method: Technician's Manual.*"

LIST OF ACRONYMS/ABBREVIATIONS/SYMBOLS

AC	Asphalt Cement
ΔH	Horizontal Deformation
ΔH_f	Fusion Enthalpy Change
ΔV	Vertical Deformation
BBR	Bending Beam Rheometer
C	Celsius
C(t)	Creep Modulus
CS	Coarse Sand
DMA	Dynamic Mechanical Analysis
DSC	Differential Scanning Calorimetry
DSR	Dynamic Shear Rheometer
EVA	Ethylene-Vinyl Acetate Copolymer
FSCH	Frequency Sweep at Constant Height test
FTIR	Fourier Transform Infrared
G*	Shear Complex Modulus
G'	Shear Storage Modulus
G"	Shear Loss Modulus
Hz	Hertz
ITS	Indirect Tensile Strength
JMF	Job Mix Formula
L	Liter
LADOTD	Louisiana Department of Transportation and Development
LTRC	Louisiana Transportation Research Center
m	Creep rate under load
M_R	Indirect Tensile Resilient Modulus
MTS	Material Testing System
N_f	Number of Cycle Times to Failure
NMR	Nuclear Magnetic Resonance
Pa	Pascal
PAC-40	Polymer modified asphalt cement equivalent to an AC-30
PAC-40HG	PAC-40 Hot Grade
PAV	Pressure Aging Vessel
PMAC	Polymer Modified Asphalt Cement
P_o	Applied Vertical Load
P_{ULT}	Ultimate Applied Load to Failure
RPMAC	Reclaimed Polymer Modified Asphalt Cement
s	Second
S(t)	Creep Stiffness
SBS	Styrene-Butadiene-Styrene Block Copolymer
SHRP	Strategic Highway Research Program
Superpave	Superior Performance Asphalt Pavements
TFOT	Thin Film Oven Test
T_g	Glass Transition

T_m	Melting Point
US-61C	Field aged binder extracted from core samples
US-61S	Field aged binder extracted from surface bump grind samples
VFA	Volume of Voids Filled with Asphalt
VMA	Volume of Voids in Mineral Aggregate
λ	Wave Length
η	Viscosity
μ	Poisson Ratio

REFERENCES

1. R.-B. Jiang, J.-D. Lin, and D.-F. Lin, "Rheology of Asphaltic Binders and Their Effects on Asphalt Concrete," *Transportation Research Record No. 1535*, Transportation Research Board, 1996.
2. Brule, B., "Polymer-modified asphalt contents used in the road construction industry: Basic principles." *Transportation Research Record No.1535*, Transportation Research Board, 48-53 (1996).
3. K.R. Wardlaw, and S. Shuler, "Polymer Modified Asphalt Binders", ASTM STP, Vol. 1108, Philadelphia, PA, 1992.
4. G.N. King, O. Harders, and P. Chavenot, "Influence of Asphalt Grade and Polymer Concentration on the High Temperature Performance of Polymer Modified Asphalt", *Proceedings of the Association of Asphalt Paving Technologists*, Vol. 61, 29-61, 1992.
5. Goodrich, J. L., "Asphalt and Polymer Modified Asphalt Properties Related to the Performance of Asphalt Concrete Mixes", *Proceedings of the Association of Asphalt Paving Technologists*, Vol. 57, 116-175, 1988.
6. Taylor, N.H., "Life Expectancy of Recycled Asphalt Paving," Recycling of Bituminous Pavements, Editor, L. E. Wood, ASTM STP 662, American Society for Testing Materials, Philadelphia, PA, 1977, pp. 3-15
7. Roberts, F. L., Kandhal, P.S., Brown, E. R., Lee, D. Y., and Kennedy, T. W., "Hot Mix Asphalt Materials, Mixture Design, and Construction," NAPA Education Foundation, Lanham, Maryland, 1991, pp. 439.
8. Nady, R. M., "The Quality of Random RAP, Separating Fact from Supposition," Focus on HMAT, Hot Mix Asphalt Technology, National Asphalt Pavement Association, Vol. 2, 1997 pp.14-17.
9. Buttlar, W.G., Bozkurt, D., Al-Khateeb, G.G., and Waldhoff, A.S. "Understanding asphalt mastic behavior through micromechanics." *Transportation Research Record 1681*, Transportation Research Board, 157-169 (1999).
10. Oliver, J.W.H., Tredrea, P.F., Witt, H.P., "Relationships Between Binder Properties and Asphalt Rutting," Asphalt & Surfacings, Stabilisation, Recycling, Vol. 2, Proceedings of Combined 18th ARRB Transport Research Conference Transit NZ Land Transport Symposium, Christchurch, New Zealand, 2-6 September 1996, pp. 149-164.
11. Blanco, R. Rodriguez, R., Garcia-Garduno, M., and Castano, V.M. "Morphology and tensile properties of styrene-butadiene copolymer reinforced asphalt." *J. Appl. Polym. Sci.*, 56, 57-64 (1995).

12. Blanco, R. Rodriguez, R., Garcia-Garduno, M., and Castano, V.M. "Rheological properties of styrene-butadiene copolymer reinforced asphalt." *J. Appl. Polym. Sci.*, 61, 1493-1501 (1996).
13. Gahvari, F. (1997). "Effects of thermoplastic block copolymers on rheology of asphalt." *J. Mater. Civ. Eng.*, 9, 111-116.
14. Green, J., Yu, S., Pearson, C. and Reynolds, J. "Analysis of Sulfur Compound Types in Asphalt," SHRP-A-667, Strategic Highway Research Program, National Research Council, Washington, DC 1993
15. AASHTO TP5 "Determining the rheological Properties of Asphalt Binder Using a Dynamic Shear Rheometer".
16. AASHTO TP1 "Determining the Flexural Creep Stiffness of Asphalt Binder Using the Bending Beam Rheometer (BBR)."
17. Mohammad, L.N. and Paul, H.R. "Evaluation of a New Indirect Tension Test Apparatus", Transportation Research Record, Vol. 1353, 1992.
18. Texas DOT, "Test Method Tex-231-F," Texas Department of Transportation, Division of Materials and Tests, Revised, Feb., 1993.
19. Mull, M.A., K. Stuart and A. Yehia, Fracture resistance characterization of chemically modified crumb rubber asphalt pavement, J. of Materials Science, Vol. 37 (2002) 557-566.
20. L. N. Mohammad, Wu, Z., Mull, M.A. (2004). "Characterization of Fracture and Fatigue Resistance on Recycled Polymer-Modified Asphalt Pavements". *Proceeding of the 5th RILEM International Conference on Pavement Cracks*, France, 2004.
21. Wu, Z., L. Mohammad, and Mull, M.A. (2004). "Characterization of Fracture Resistance of Superpave Mixture using the Semi-Circular Bending Test," *Journal of ASTM International (JAI)* (in print).
22. Fan, S and Kyu, T., "Reaction Kinetics of Thermoxidative Degradation in a Styrene-b-butadiene Diblock Copolymer" *Macromolecules*, 34, 645-649 (2001).
23. Noel, F. and Corbett, L. W. "Crystalline Phase in Asphalts" *Journal of the Institute of Petroleum*, Vol. 56, 1970, pp. 261-268.
24. H. K. Huynh, H. K., Khong, T. D., Malhotra, S. L. and Blanchard, L., "Effect of Molecular Weight and Composition on the Glass Transition Temperature of Asphalts" *Analytical Chemistry*, Vol. 50, 1978, pp. 976-979.
25. B. Brule, B. Planche, J. P., King, G., Claudy, P. and Letoffe, J. M., "Characterization of Paving Asphalts by Differential Scanning Calorimetry", *Fuel Science & Technology International*, Vol. 9, 1991, pp. 71-92.

26. Daly, W.H., Qiu(Chiu), Z.-Y. and Negulescu, I.I., “Differential Scanning Calorimetry Study of Asphalt Crystallinity" *Transportation Research Record No. 1535*: Transportation Research Board p. 54-60 (1996).
27. Mohammad, L.N., Negulescu, I., Wu, Z., Daranga, C., Daly, W.H., and Abadie, C., "Investigation of the Use of Recycled Polymer Modified Asphalt Binder in Asphalt Concrete Pavements," *Journal of the Association of Asphalt Paving Technologist*, 2003, pp. 551-594.
28. Bhurke, AS; Shin, EE; Drzal, LT. “Fracture Morphology and Fracture Toughness Measurement of Polymer- modified Asphalt Concrete,” Journal of the Transportation Research Record No. 1590, 1996.
29. Petersen, J.C. Fuel Sci. Technolo. Int., 110: 57 (1993).
30. Tropsha, Y. and A. Anthony, Photodegradation of Asphalt and its Sensitivity to the Different Wavelengths of the Sunlight Spectrum, Proc. ACS Div. Polym Mater., 66, (1992) 305
31. Mill, T., D.S. Tse, B. Loo, C.C.D. Yao and E. Canavesi, "Oxidation Pathways for Asphalt," Prepr. ACS Div. Fuel Chem., 37(3) (1992) 1367.
32. Huang, J. "Oxidation of Asphalt Fractions," in Asphalt Science and Technology, A. Usmani ed. Marcel Dekker, New York, 1997, 119-134.
33. Aglan, H. A. Othman, L. Figueroa and R. Rollings, "Effect of Styrene-Butadiene-Styrene Block Copolymer on Fatigue Crack Propagation Behavior of Asphalt Concrete Mixtures," Transportation Research Record 1417, Transportation Research Board, National Academy Press, Washington, D.C. 1993, 178-186.